ON THE SLIDING PRINCIPLE OF MICRO-FLUIDIC DEVICES FOR A POTENTIAL USE IN SORTING CELLS OF DIFFERENT SIZES WITH ONE DEVICE

A Thesis Submitted to the

College of Graduate and Postdoctoral Studies

in Partial Fulfillment of the Requirements

for the Degree of Master of Science

in the Division of Biomedical Engineering

University of Saskatchewan

Saskatoon

by

ANNAL ARUMUGAM ARTHANARI ARUMUGAM

PERMISSION TO USE

In presenting this thesis in partial fulfillment of the requirements for a Postgraduate degree from the University of Saskatchewan, I agree that the Libraries of this University may make it freely available for inspection. I further agree that permission for copying of this thesis in any manner, in whole or in part, for scholarly purposes may be granted by the professor or professors who supervised my thesis work or, in their absence, by the Division of Biomedical Engineering or the Dean of the College of Graduate and Postdoctoral studies at the University of Saskatchewan. It is understood that any copying or publication or use of this thesis or parts thereof for financial gain shall not be allowed without my written permission. It is also understood that due recognition shall be given to me and to the University of Saskatchewan in any scholarly use which may be made of any material in my thesis.

Requests for permission to copy or to make other use of material in this thesis in whole or part should be addressed to:

Division of Biomedical Engineering

University of Saskatchewan

57 Campus Drive,

Saskatoon, Canada

SK S7N 5A9

OR

Dean

College of Graduate and Postdoctoral Studies

University of Saskatchewan

116 Thorvaldson Building, 110 Science Place

Saskatoon, Saskatchewan S7N 5C9 Canada

ABSTRACT

In recent times, numerous microfluidic devices have been developed to assist in cell analysis both in research and clinical units. Different microfluidic devices capable of capturing, isolating, positioning and sorting single cells have been developed. However, these devices are incapable of working with cells of different sizes; in particular, one device can only work for cells of one size. This problem was addressed in literature with the concept called adaptable or tunable device. Such a device can capture and sort single cells of different sizes, ranging from 20 to 30 µm, due to the inherent limitation of the working principle behind such a device (i.e., deformation-based adjustment of the geometry of the device). On the other hand, in many applications, the desired size range is expected from 2 µm to 100 µm or more.

This thesis first conducted an analysis of different working principles of devices for capturing and sorting single cells, attempting a solution to the problem. As a result, this thesis proposed a novel principle for devices to perform sorting single cells with the cell size ranging from 2 µm to 100 µm, and this principle is named “sliding principle”. To prove the sliding principle to work, a device that contains a micro-trapper or well based on this principle was designed and fabricated using soft lithography with the mold fabricated with a 3D printing technology. The experiment conducted with the microscopy (resolution: 1-3 micron) and motion stage (resolution: 1 micron), which shows that the device can adjust the size of the well trapper, ranging from 0 to 1000 µm and covering the desired cell size range (i.e., 2 µm to 100 µm). According to the current literature on the mechanical approach to capture and sort single cells of different sizes with one device,

the device built based on the sliding principle should potentially be applicable to capturing and sorting single cells of different sizes with one device.

This study has a few limitations: (1) the accuracy of the device is not good enough due to the interaction of the PDMS membrane and the model; (2) the inlet and outlet for fluids were not taken in the scope of this research owing to the difficulty of getting proper microspheres or cells for subsequent directing testing on the device. However, the outcome of the present study has paved the way for future research to overcome the preceding limitations.

The main contribution of this thesis is the provision of a new design concept, namely “sliding principle” in the field of micro-fluidic system, for tunable or flexible micro-fluidic devices for a potential application in the tasks such as capturing and sorting single cells of different sizes. In a long run, the sliding principle is a first step towards a new approach to micro-fluidic systems called “robotic micro-fluidic systems”, which adds intelligence to a micro-fluidic system.

ACKNOWLEDGMENTS

I would like to express my deepest appreciation and gratitude to my supervisor, Professor Chris Zhang, for his great support during my academic studies and research. He has been a great source of knowledge and has inspired me in various ideas which are significant for my research. The useful discussion and advice from him during our meetings made my studies and research flow smoothly. This thesis cannot be finished without his meticulous reviews.

My special thanks go to Anthony Tony for his committed tutoring during my research period. His open-minded thoughts and discussions helped me to shape my skills of understanding research problems in a practical way.

I would also like to thank scientist Garth wells and Michael Jacobs in SyLMAND (Canadian light source) who guided me in various ways during the fabrication process.

TABLE OF CONTENTS

LIST OF FIGURES

CHAPTER 1

INTRODUCTION

1.1 Background

Manipulation and control of flow of fluids in channels with a dimension from tens to hundreds of micrometers is a subject of knowledge, which is embraced in microfluidics and has emerged as a distinct field in the recent years. Microfluidics has its significance over the application areas from chemical synthesis, biological analysis to optics and information technology (Whitesides, 2006). Many microfluidic devices have been developed to assist in cell analysis, which has produced a huge benefit to these application areas (e.g., medical area). A generic function for all these tasks concerning cells is the device that can capture single cells of different sizes. This function is called single cell capturing in this thesis.

The microfluidic technology has proven its functional advantage over the conventional cellomics methods such as flow cytometry (FC) and laser scanning cytometry (LSC) for analysis of single cells (Soberanes et al., 2016). Different microfluidic devices capable of capturing, positioning, and sorting single cells have been developed with principles such as electrical, magnetic, optical, and mechanical manipulation (Yi et al., 2006). However, such devices are incapable of working with cells of different sizes (Soberanes et al., 2016); in particular one device can only work for cells of one size. This problem was addressed in literature with the concept called adaptable or tunable

device (Zhu et al., 2014). An adaptable device can only achieve the size of cells, ranging from 20 to 30 μm, due to the inherent limitation of the principle behind such a device (i.e., deformation-based adjustment of the geometry of the device), small deformation in particular. On the other hand, in many applications, the desired size range is from 2 μm to 100 μm or more. For instance, even the same cells may have a different diameter during their growth, e.g., MCF-cells (Human breast cancer cells) are with the average diameter of 20 μm - 24 μm, chlorella cells with the average diameter of 2 μm - 5μm, MCS (mesenchymal stem cells) with the average diameter of 14 μm and ESC (Human embryo stem cells) with the average diameter of 10 μm – 20 μm (Lawrenz et al., 2012). So, there was a high desire to develop one device that can capture single cells with their size ranging from 2 μm to 100 μm or more. Such a device is called an adaptable device.

1.2 Adaptable devices for single cell capturing

The adaptable devices are built based on the principle of deforming a trapper or channel. One can design a device that contains many trappers (Fig. 1.1). When cells flow over the device, cells are expected to drop into the trappers. To trap cells of different sizes, the size of the trappers needs to be changed, which can be achieved by imposing forces on the device. There are several developments of cell trappers based on this principle, such as (1) the device made by Huh et al. (2007) which has nano-size channel and the corss section area of the channel can be changed by the lateral compression, (2) the device made by (Beech & Tegenfeldt, 2008), which has the channels, and their lateral dimension can be changed by the stretching force perpendicular to the cross-section area of the channel, and (3) the devices made by Zhu et al. (2014) and

Soberanes et al. (2016), in which the trappers are like wells rather than channels. The inherent limitation of this device principle is its small deformation, which is further translated to the limitation that only a small cell size range (about 10 µm) can be achieved.

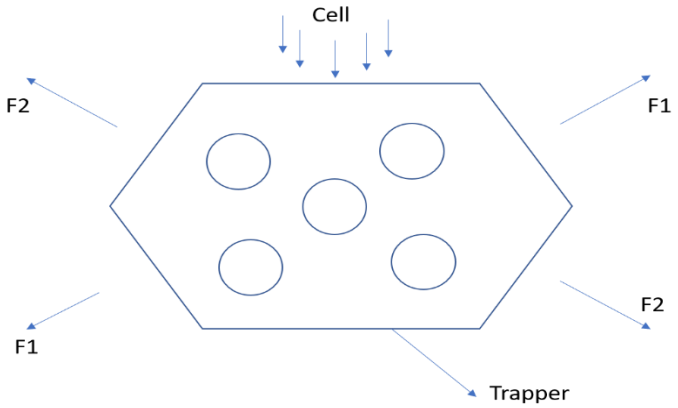

Fig. 1.1 Adaptable devices with force imposed on trapper.

1.3 Research Question

2-5 µm? Is it possible to design and fabricate a microfluidic trapper which can capture or sort a single cell, the size of which ranges from 2 µ to 100 µ or more with the size resolution being

1.4 Research Objectives

This thesis was defined to provide an answer to the above question. The overall objective of the thesis was to develop a new microfluidic device with trappers being modified in accordance with the size of cells, ranging from 2 µm to 100 µm with the size resolution of 2-5 µm). The general idea in this thesis is to develop the trapper into a sort of mechanism with sliding elements in it

and changing the size of the trapper by operating the sliding element (Fig. 1.2). In Fig. 1.2, the trapper is of a square shape and the change of its size is made by changing the edge of the square (Fig. 1.2a). This means that the edge of the square is made as sliding. Overall, the trapper is like a mechanism which has four movable edges. This concept of the trapper is called sliding principle and it was studied in this thesis. This thesis further considers that only one edge can be slidable without loss of generality (Fig. 1.2b).

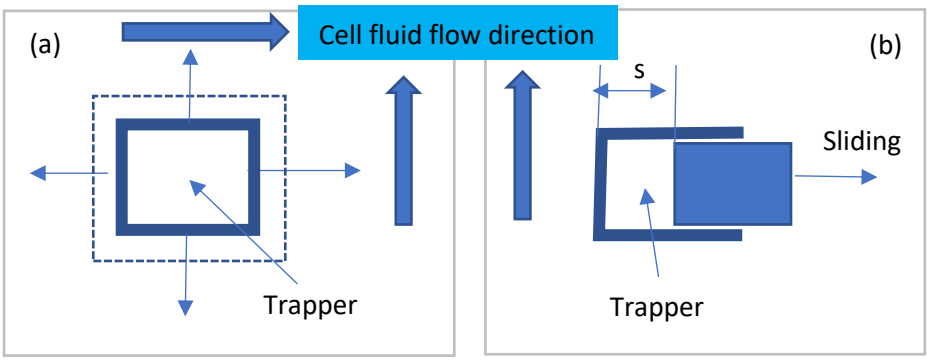

Fig. 1.2 The sliding principle of the adaptable trapper. (a) The trapper is a square with four edges that can be slide. (b) The one edge is sliding to change the size of the trappers, i.e., s.

Considering the above discussion, the specific objectives of this thesis were defined as follows:

- **Objective 1**: Classify and compare the existing principles of devices for single cell capturing and sorting to come up with their pros and cons and to consolidate the sliding principle.
- **Objective 2**: Develop the prototype of a device based on the sliding principle to explore the effectiveness of this principle as well as its limitation.

This thesis did not test the device on biological cells or chemical microspheres due to the limited resource available as well as the consideration that the success of such testing is much dependent on the success of whether the trapper can be changed in its size with the sliding principle. Indeed, the previous student in our group successfully tested on cells with the tunable device with the deformation principle. In principle, the device based on the sliding principle should create less stress on cells than the device based on the deformation principle, so the success of the testing on cells with the device based on the sliding principle should be very high. Further, in this thesis, capturing and sorting of cells of different sizes are used interchangeable, though capturing is a kind of sorting.

1.5 Organization of the thesis

The organization of the thesis is as follows. Chapter 2 provides a critical literature review on the different principles of devices for single cell capturing by following the methodology proposed in literature (Li et al., 2015). Chapter 2 also presents the general design theory and methodology, which was applied to design the device based on the sliding principle. The last section of Chapter 2 further argues the promise of the sliding principle. Chapter 3 presents the design of the device based on the sliding principle, which includes the embodiment and detail design. In Chapter 4, the fabrication of the device based on the sliding principle is presented. Chapter 5 presents the testing of the device. In Chapter 6, concluding remarks along with a discussion of how the objective of the research is achieved. There is also a discussion of the limitation of the sliding principle and of some future work.

CHAPTER 2

BACKGROUND AND LITERATURE REVIEW

2.1 Introduction

In this chapter, further background and literature review are presented. Section 2.2 presents a detailed review and classification of the principles of devices that can potentially perform single cells capturing (and thus sorting) to reveal the state of arts of device technology for one device to capture cells with different sizes. Section 2.3 describes some existing adjustable microfluidic devices with different techniques, which were employed to make a prototype of the new device. Section 2.4 describes some design theories and methodologies, which were employed in conducting the design of a device to capture single cells with different sizes. Finally, Section 2.5 gives a conclusion regarding the need for and urgency of this thesis research.

2.2 Principles of devices for single cell capturing

The principle is the fundamental law that governs the behaviour, which exhibits a relationship among a set of variables (Zhang et al., 2005). To be able to capture cells of different sizes, the requirement is that cells can be separated based on their sizes. There are five principles of devices that meet the requirement – i.e. to capture single cells: electrical manipulation, magnetic manipulation, optic manipulation, acoustic manipulation, and mechanical manipulation. In the

following, the potential of developing devices based on these principles for one device to capture single cells of different sizes is discussed. A care must be taken about the sense of capturing single cells of different sizes. First, single cells are captured rather than a granular of cells is captured. Second, to a group of cells of different sizes, a device can be adjusted such that in one state of the device, cells of size X are captured individually, and in another state, cells of size Y are captured individually.

2.2.1 Magnetic Manipulation

Microfluidic devices, in which cells are trapped by the external appliance of the magnetic field, are based on the magnetic manipulation principle. In this principle, magnetic particles are attached to cells so that they can respond to an external magnetic field (Yi et al., 2006). The super-paramagnetic beads with 10-100 nm diameter are used for example in the device, as shown in Fig. 2.1. In Fig. 2.1, ferromagnetic wires are counter-sunk into the bottom of the chamber with 45° angle and more than 350 channels are aligned for cell flow. Cells receive a magnetic force to be pushed to flow along the wire, as the closer to the wire, the higher the magnetic field intensity. Magnetophoretic separation of red blood and white blood cells is achieved with a device based on this principle (Han & Bruno Frazier, 2004).

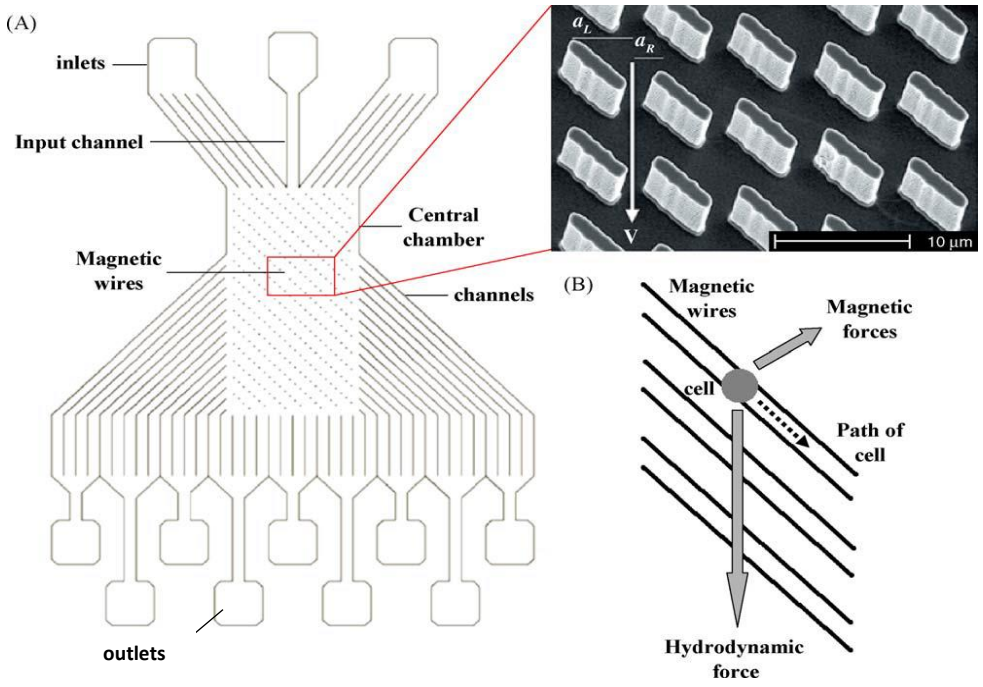

Fig. 2.1 Micro-fabricated device with magnetic wires and magnetic force separation (Yi et al., 2006, p.3).

The device built based on this principle is versatile, non-invasive and clean (Yi et al., 2006). However, this principle cannot capture single cells of different sizes, because the principle has nothing to do with the size of cells but has something to do with the number of magnetic particles attached on the cells. It is possible that a large size cell can attach a huge number of magnetic particles, and as such, the force received by the large size cell with the magnetic particle attachment is higher and thus the cell moves faster. By this technique, separation of large size cells from small size cells is possible based on their different motions. However, first, it is not clear at present the attachment capacity has a causal relation with the size of cells, and second, the resolution in the size of cells to be separated is likely not very high. In addition to the foregoing uncertainty, the approach is too complicated.

2.2.2 Electrical Manipulation

The electrical manipulation principle refers to the device in which cells are sorted or trapped by applying an external electric field on cells. The principle is based on another physics that is the effect of Dielectrophoresis (DEP), which says a force is exerted on a dielectric substance when it is exposed to a non-uniform electric field (wiki: https://en.wikipedia.org/wiki/Dielectrophoresis). Given the same electric field and frequency, the force depends on the shape and size of cells (wiki: https://en.wikipedia.org/wiki/Dielectrophoresis). Therefore, it is possible to capture cells of different sizes or sort cells in terms of their sizes. However, the approach based on this principle to separate cells in terms of their size involves a very complicated process and instrumentation setup. In addition, the resolution in the size of cells to be separated is likely not very high.

2.2.3 Optical Manipulation

According to (http://www.sciencebriefss.com/dictionary/optical-tweezers-definition-science-terms-explained), optical tweezer, which is also known as “single-beam gradient force trap”, uses a highly focused laser beam to create a gradient electric field. When cells or more generally dielectric particles flow to the field, they tend to be trapped into the center of the field. The flow rate of cell fluids depends on (1) the relative refractive index, a ratio of the speed of light from one medium to another (between the cell fluid and the environment), and (2) the strength of the field or the gradient force. These two have a relationship. Since different cells have different

relative refractive index, they can be separated based on their different flow rates with same gradient force.

Cells of different sizes may have different relative refractive indexes. As such, the optical tweezer may be utilized to sort cells of different sizes. However, the relative refractive index may depend on several factors including the size. That said; the relative refractive index and size of cells are not a one-to-one relation. Therefore, separation of cells based on the relative refractive index will inherently be restricted in terms of accuracy.

2.2.4 Acoustic (ultrasonic sound) Manipulation

The principle of the technique is based on the effect known as acoustic streaming (https://en.wikipedia.org/wiki/Acoustic_streaming). When an acoustic wave travels along a water-coated surface, the wave will trigger the droplets inside the water to deflect the stream of droplets. This technique can then be applied to sort cells — i.e. to separate cells from medium or "waste". Franke et al. (2010) proposed a system, which is based on this principle, to sort cells (Fig. 2.2). The device is designed such that the left channel has less resistance to the fluid movement. Therefore, without activating the surface acoustic wave on the channel, the cell fluid will just move along the left channel. However, when the surface acoustic wave is activated, the acoustic streaming effect causes the cells turn to the right channel. By that, cells are separated from the medium. This principle is difficult to make a device to capture cells of different sizes,

because the size of cells does not explicitly relate the behaviour of streaming (e.g., trajectory of the streaming).

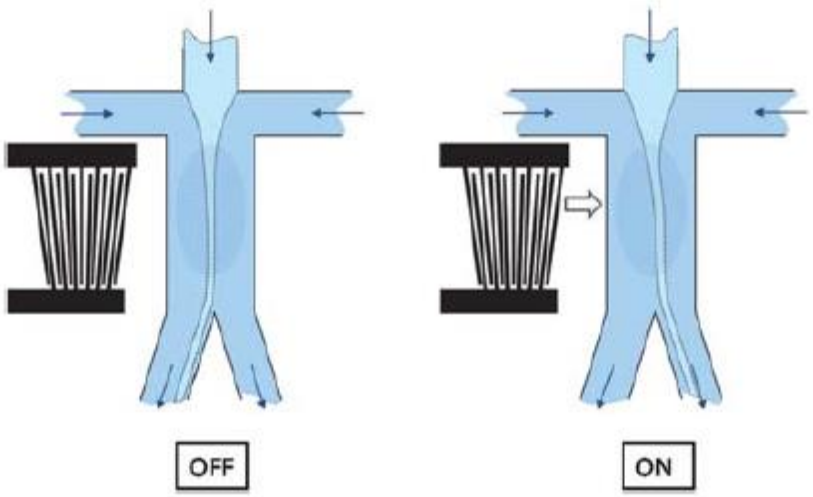

Fig. 2.2 SAW sorting by electronic control (Franke et al., 2010, p.790).

2.2.5 Mechanical Manipulation

The principle of devices called mechanical manipulation is to provide geometry to a device such that cells get trapped due to the geometric constraint while cell fluids flow over the device. The geometrical features lead to the devices such as microfilters (Fig. 2.3A), microwells (Fig. 2.3B), microgripper (Fig. 2.3C), sandbag structure (Fig. 2.3D), dam structure (Fig. 2.3E) and variable microchannel interior surface (Yi et al., 2006; Zheng et al., 2007).

Another micro-well structure is shown in Fig. 2.4, where there is a membrane with an array of conical nanopores on it, called a conical nanoporous membrane (CNM), which is placed between a top layer and a bottom layer (Guo et al., 2012). Each conical nanopore has an identical base

diameter of 1 µm and tip diameter of 500 nm. The flow is created with a negative pressure (2000pa).

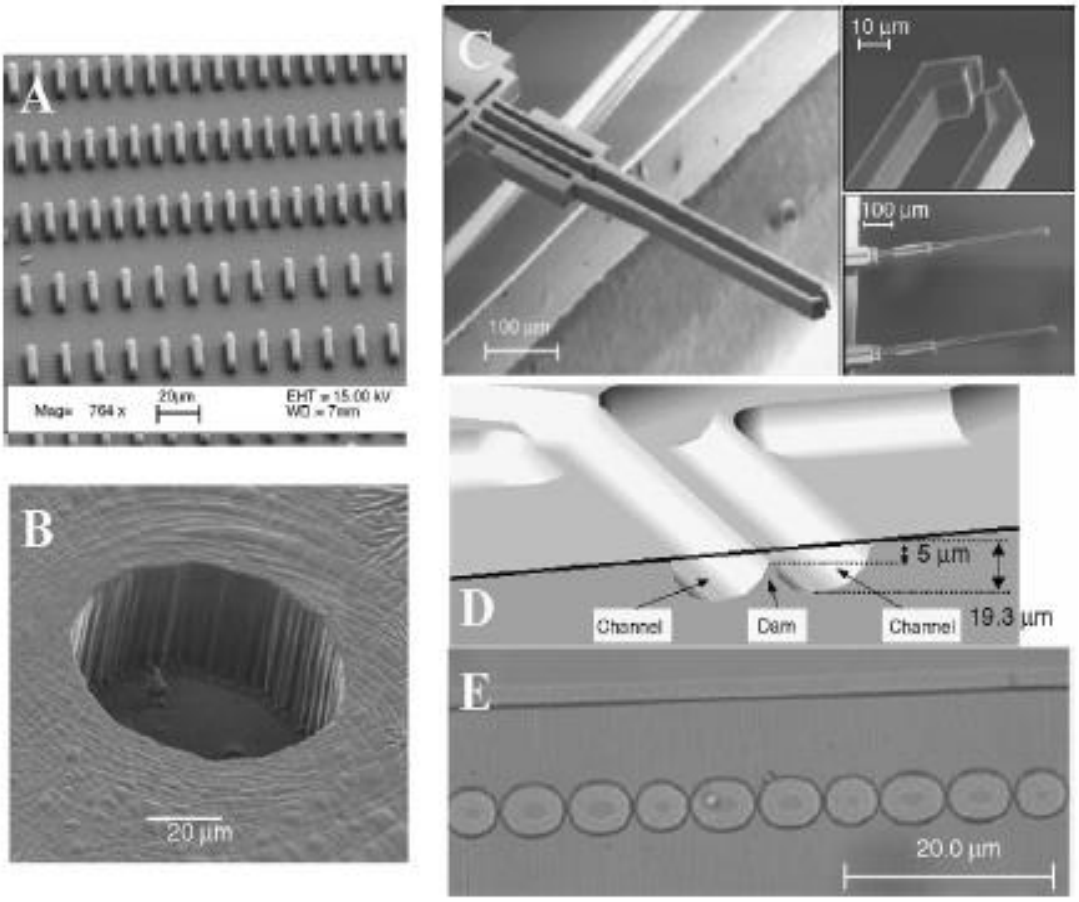

Fig. 2.3 Different types of devices that have different ways to create a geometric constraint (Yi et al., 2006, p.5).

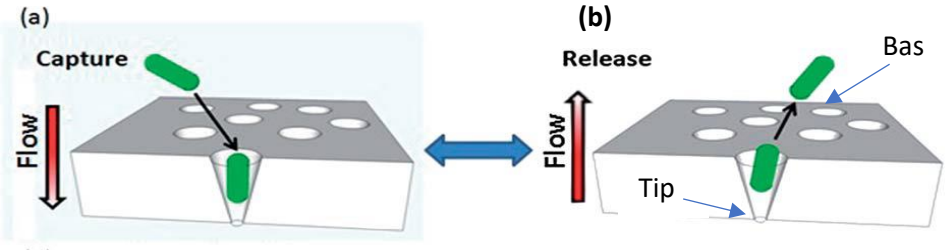

Fig. 2.4 Capture and release of CNM (Guo et al., 2012, p.559).

Fig. 2.5 shows yet another device with a concept called growth channels – i.e. channels with different widths from 0.3 µm, 0.4 µm up to 0.8 µm, which are made in parallel to one another. A trench passes through the parallel growth channels, in which cells flow. Cells grow in different sizes, and then get trapped into different growth channels.

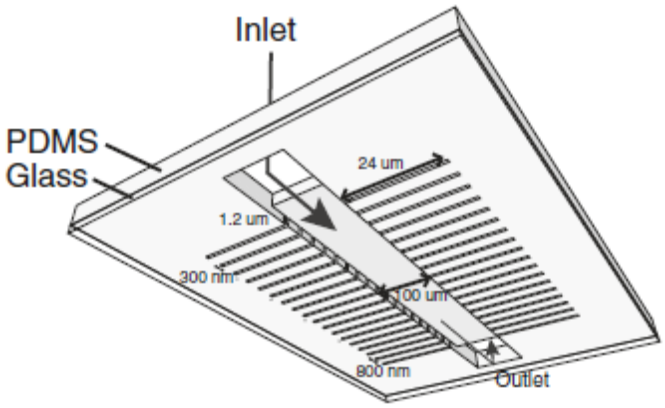

Fig. 2.5 Microfluidic device with growth channels (Moolman et al., 2013, P.2).

2.3 Capability of one device to capture cells with different sizes in mechanical manipulation

The discussion in Section 2.2 shows that the mechanical manipulation principle is the most promising approach to capture different cells with one device. In the existing literature, the basic approach is to deform the trap to increase its size to accommodate cells with different sizes. The first attempt with this approach was made by Huh et al. (2007); see Fig. 2.6, where an array of parallel nano-channels is made on; in particular the channel is with the shape of isosceles and its length of 688±79nm and its width of 78±18 nm. The compression force is applied perpendicular to the channels. Fig. 2.7 shows a device developed by Beech & Tegenfeldt (2008) using the elasticity of PDMS. The stretching force is applied to the lateral direction of the channels. The

change can reach 50% of the original size, the cell size ranges from 60 nm to 96 nm with a resolution of 18 nm.

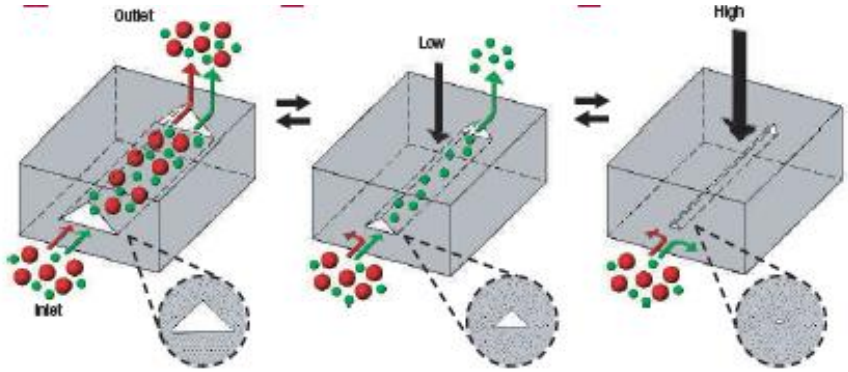

Fig. 2.6 Flexible elastomeric nanochannels (Huh et al., 2007, p.425).

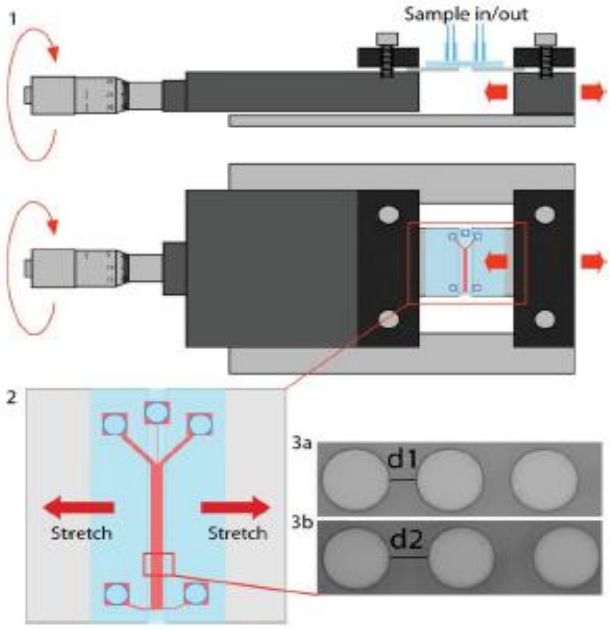

Fig. 2.7 Particle separation by tuning (Beech & Tegenfeldt, 2008, p.658).

In advancing this deformation-based approach, Zhu et al. (2014) and Soberanes et al. (2016) proposed a well-line trapper instead of the channels. The well-like trapper tends to be more uniformly deformed; besides the flow direction can be in many directions instead of one direction

(i.e., along with the channel direction). Fig. 2.8 shows the device developed by Soberanes et al. (2016). The device consists of two thin sheets of the elastomer PDMS, where the bottom layer has an array of microstructures protruded on its surface. The device of Zhu et al. (2014) can achieve the cell size range of 18μ to 28μ with a resolution of 0.8μ. The device of Soberanes et al. (2016) can achieve the cell size range of 20μ to 30μ with a resolution of 2μ.

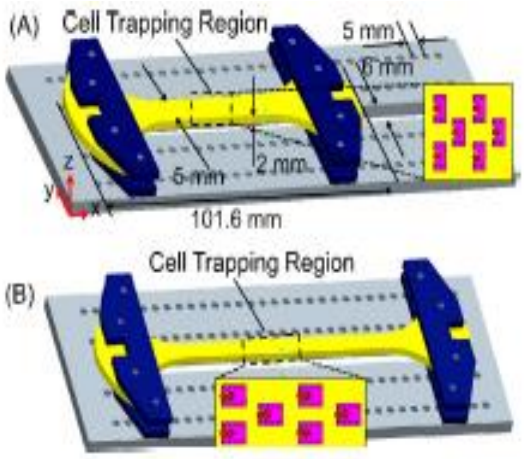

Fig. 2.8 Adaptable single cell trapper (Soberanes et al., 2016, p.35).

For the deformation-based method, the external force field can be generated by a piezoelectric actuator (Graf & Bowser, 2008), a pneumatic actuator (Tice, Bassett, Desai, Apblett, & Kenis, 2013), and dielectric polymer actuator (Murray et al., 2013). The major drawbacks of these devices are higher cost, more complicated fabrication, non-uniform change of the size of channel or trapper at a certain point of deformation, and perhaps contamination to cells with either electrical or pneumatic connection.

Chang et al. (2015) proposed a new mechanical principle of devices that allow changing the topology of the device and changing the size of the channel. The principle is the sliding principle, as illustrated in Fig. 2.9. In Fig. 2.9, there are two PDMS layers, each of which contains a few channels, and the two PDMS layers slide against each other in a certain type of movements (rotation, translation, general motion), e.g., the upper block translates over the bottom block in the case of Fig. 2.9. Fig. 2.9(a) shows how the topology (i.e., connectivity) of the two-layer system is changed, and Fig. 2.9(b) shows how the size of the channel is changed. In principle, the concept of Chang et al. (2015) should be possibly used for one device to capture single cells of different sizes.

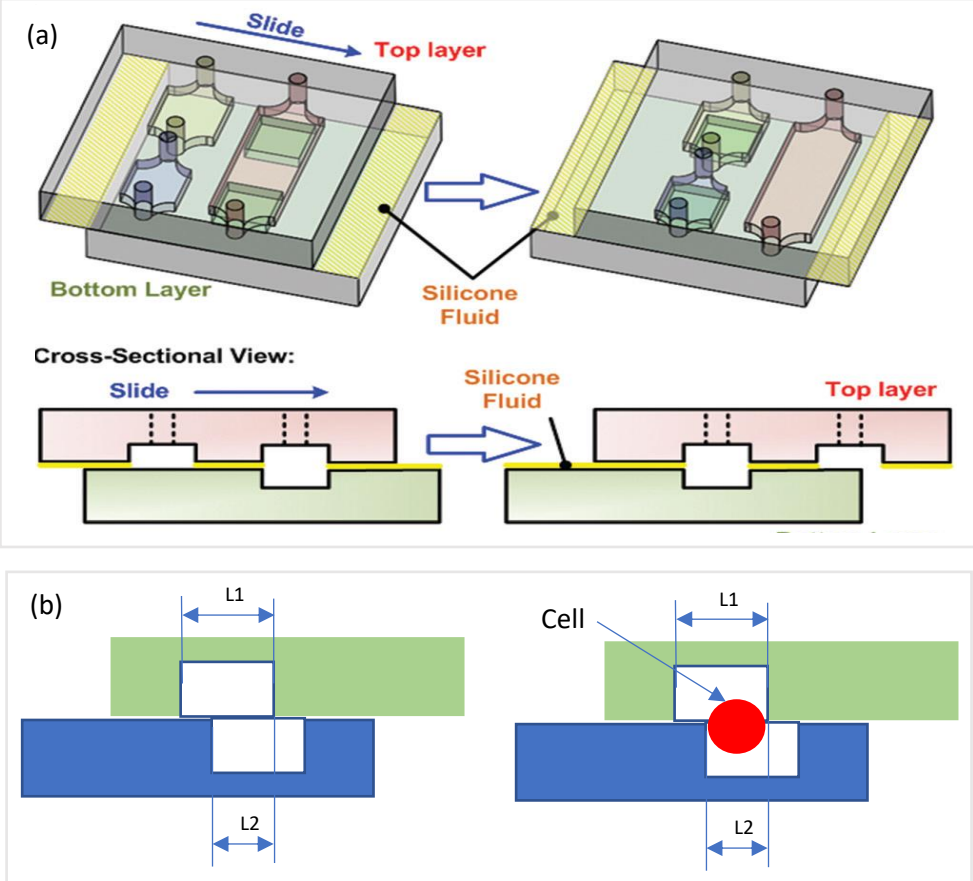

Fig. 2.9 PDMS slip chip to culture cells (Chang et al., 2015, p.7357).

In realizing the above concept of Chang et al. (2015), there is also a layer of material, Si-fluid, put between the two blocks, which has two roles: sealing and lubricating. The device is fabricated by using soft lithography replica molding process and the master mold is fabricated by a negative tone photoresist. The Si-fluid is composed of dimethyl siloxane and tri-methyl-siloxane-terminated silicone, which has a viscosity of 10 000cSt. The resulting thickness of the Si-fluid layer obtained is less than 9 μm. The device was treated with oxygen plasma to make the channel surface hydrophilic, and biocompatibility was tested with A549 and MCR-5 cells (Chang et al., 2015).

2.4 Design theories and methodologies

Two general design theories and methodologies were employed in this thesis, including: (1) general design phase theory, and (2) axiomatic design theory — Axiom 1 in this case. These theories are described below.

2.4.1 General design phase theory

According to Zhang (2017), design can be divided into four general phases: (1) technical specification of customer requirements, (2) concept design, (3) embodiment Design, and (4) detail design.

The task at the phase (1) is to develop a complete description of the requirements for a device or system under design with technical terms. For instance, the consumer voice of requirement may be ‘penetrate common metal’. This requirement may be described in the technical specification as ‘penetrate materials with their hardness measure HRC>35’, where HRC is a type of measures for material hardness. According to Zhang (2017), a relatively formal method can be used to write the technical specification. FR: function requirement, CR: constraint requirement, and PR: performance requirement, and R: requirement. Further, R (FR, CR, PR) may be decomposed into simpler ones, e.g., FR may be decomposed into FR1.1, FR1.2, where the first number ‘1’ stands for the 1st level, and the second number ‘2’ stands for the second function requirement; together FR1.2 means the function requirement at the 1st level and 2nd position. The task at the phase (2) is to determine the principle of devices that can meet the requirements. For instance, the deformation-based approach to change the channel size is a principle of devices that can change the channel size. The task at the phase (3) is to materialize each concept and to determine the geometry to each concept and to determine spatial and temporal relations among a set of concepts. The task at the detail design phase (4) is to modify the geometry and surface quality of each component considering the manufacturability of each component and eventually the whole system.

2.4.2 Axiomatic design theory

The axiomatic design theory (ADT) (Suh, 1990) involves two axioms which are expected to make a better design. In this thesis, Axiom 1 has been employed. The following is a description of Axiom 1, cited from the reference of (Suh, 1990) and the reference of (Fan et al., 2015).

Axiom 1: (1) FRs (at the leave of a function decomposition hierarchy) should be independent to each other; (2) DPs should maintain the independence of FRs.

A note is taken care of (2). There are three situations related to (2). The first situation is that DP has a one-to-one relation to FR, see Fig. 2.10a.

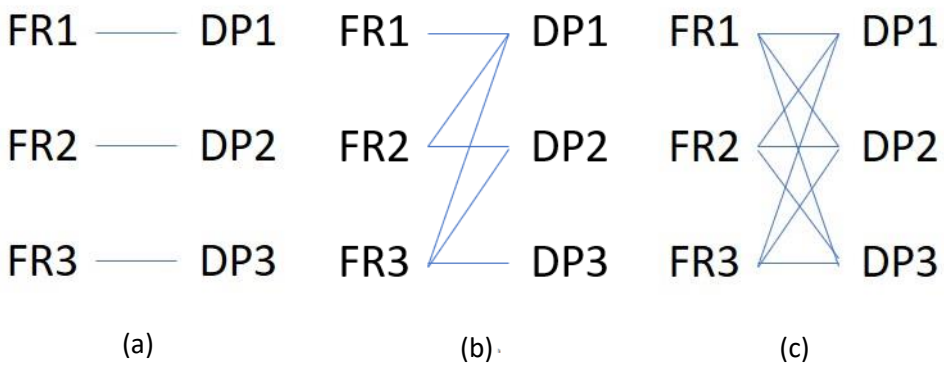

Fig. 2.10 Correspondence between FRs and DPs. (a) uncoupled, (b) decoupled, (c) fully coupled.

Mathematically, this correspondence between DP and FR can be expressed by

$$\begin{bmatrix} FR1 \\ FR2 \\ FR3 \end{bmatrix} = \begin{bmatrix} A11 & 0 & 0 \\ 0 & A22 & 0 \\ 0 & 0 & A33 \end{bmatrix} \begin{bmatrix} DP1 \\ DP2 \\ DP3 \end{bmatrix} \quad (3.1)$$

The above correspondence is called uncoupled design.

The second situation is that DP has a one-to-many relation, see Fig. 2.10b. Mathematically, this correspondence between DP and FR can be expressed by

$$\begin{bmatrix} FR1 \\ FR2 \\ FR3 \end{bmatrix} = \begin{bmatrix} A11 & 0 & 0 \\ A21 & A22 & 0 \\ A31 & A32 & A33 \end{bmatrix} \begin{bmatrix} DP1 \\ DP2 \\ DP3 \end{bmatrix} \quad (3.2)$$

This correspondence is called a decoupled design.

The third situation is that DP has a many-to-many relation with FR, see Fig. 2.10c. Mathematically, this correspondence between DP and FR can be expressed by

$$\begin{bmatrix} FR1 \\ FR2 \\ FR3 \end{bmatrix} = \begin{bmatrix} A11 & A12 & A13 \\ A21 & A22 & A23 \\ A31 & A32 & A33 \end{bmatrix} \begin{bmatrix} DP1 \\ DP2 \\ DP3 \end{bmatrix} \quad (3.3)$$

It is noted that the many-to-many relation may not be a full coupling, but it is certainly neither an uncoupling nor a decoupling.

2.5 Conclusion

Based on the review and analysis of the literature, it can be concluded that there is still room to advance the technology for one device to capture single cells of different sizes. The principle of devices, sliding principle, should be promising, as the work of Chang et al. (2015) has provided a proof of this concept. However, the work of Chang et al. (2015) is about the channel. This thesis was expected to explore the well, explicitly changing the size of well based on the sliding principle, and it is worthy of the effort to develop a prototype to test the concept of this thesis.

CHAPTER 3

DESIGN AND ANALYSIS

3.1 Introduction

This chapter will present the design of the novel device based on the sliding principle. The design process of this device follows what was reviewed in Chapter 2. Particularly, the first step of design is to develop a technical specification, which is about the functional requirement and constraint requirement in the technical term (in Section 3.2). The second step is conceptual design (in Section 3.3). The last step is embodiment and detailed design (in Section 3.4). Section 3.5 gives a conclusion.

3.2 Technical Specification

The overall function requirement (FR) for a device is to capture cells of different sizes (from 2 µ to 100 µ with the size resolution of 2-5 µm). The overall FR is decomposed into sub-function requirements:

- FR 1: to form a sliding pair such that the trapper changes the size by sliding movement. The performance associated with the FR 1 is: 2 µ to 100 µ with the size resolution of 2-5 µm.

- FR 2: to execute the sliding trapper.
- FR 3: to pump cell fluids to flow over the trapper.

There are several constraints on the device when the device performs the above function, which are:

- CR 1: the material of the device that contacts cells must be biocompatible, which is a constraint to all the functional requirements.
- CR 2: the adjusting range of the sliding is less than 1000 μm, which is applied to FR 1 and FR 2. It is noted that the 1000 μm is taken here instead of 100 μm, as some applications involve cells which are larger than 100 μm.
- CR 3: cells should be sealed, which is a constraint to all the functional requirements.
- CR 4: multiple trappers can be put in place, which is a constraint to all the functional requirements. However, in this thesis, only one trapper is considered, as the situation of more trappers can be easily extended.
- CR 5: the maximal stress in the cell should be less than 4.5 Pa (Dimmeler, Haendeler, Rippmann, Nehls, & Zeiher, 1996), which is a constraint to all the functional requirements.

3.3 Conceptual Design

- DP 1: slot and block.

- DP 2a: two blocks with channels against each other and with relative sliding, which changes the size of channels for cells like the one of Chang et al. (2015).
- DP 2b: two blocks (upper and bottom) with rail to have the upper slide over the bottom, forming a well-like trapper like the ones developed by Zhu et al. (2014) and Soberanes et al. (2016) (see also Fig. 1.2).
- DP 3: side channel connected to the trapper (see also Fig. 1.2).

There are two design options for FR 2. Therefore, to the whole system, there are two design options. Their design matrices are represented by the following equations, respectively.

$$\begin{bmatrix} FR1 \\ FR2 \\ FR3 \end{bmatrix} = \begin{bmatrix} A11 & 0 & 0 \\ 0 & A22 & 0 \\ 0 & 0 & A33 \end{bmatrix} \begin{bmatrix} DP1 \\ DP2a \\ DP3 \end{bmatrix} \quad \text{Design option I} \tag{3.1}$$

$$\begin{bmatrix} FR1 \\ FR2 \\ FR3 \end{bmatrix} = \begin{bmatrix} A11 & 0 & 0 \\ 0 & A22 & 0 \\ 0 & 0 & A33 \end{bmatrix} \begin{bmatrix} DP1 \\ DP2b \\ DP3 \end{bmatrix} \quad \text{Design option II} \tag{3.2}$$

The two design options are uncoupled and are acceptable at this point of design according to Axiom 1 of ADT (Suh, 1990). The two design options are thus moved to the next design phase (embodiment design and detail design), and the final choice of the one will be made at there. It is noted that the constraint requirements will also be considered at the embodiment design or detail design phase.

3.4 Embodiment and Detailed design

According to the discussion in Section 2.4.2, after the concept design, it will be the embodiment design and detail design, where the material, size and spatial and temporary relation of components based on the outcome of the concept design are discussed.

3.4.1 Design option I

Fig. 3.1 shows an embodiment design to realize the design concept (Design option I, referring to DP2a in the previous discussion in Section 3.3). There are two blocks (left-hand block and right-hand block, i.e., LH and RH for short), each of which contains channels. One block is stationary and the other slides over it (see the left-lower corner in Fig. 3.1). This embodiment design is close to the one of Chang et al. (2015) but differs from their device in the area of contact between two blocks: this thesis (see the left-lower corner in Fig. 3.1) and their device (Fig. 2.9).

The embodiment design of Fig. 3.1 was attempted for fabrication, but the result was estimated to be questionable; specifically, the contact surface (Fig. 3.1) of two blocks may not be flat enough to warrant a smooth sliding between two blocks (LH, RH). Besides, the assembly of LH and RH may be difficult to meet the alignment accuracy due to its micro-dimensions. Leakage between the two blocks on the contact surface is also possible. The potential leakage problem was confirmed by simulation of the pressure distribution with the finite element method; the result is shown in Fig. 3.2. Details of the finite element model can be found in Appendix B. The result

shows from Fig. 3.2 that the maximum pressure occurs on the contact surface, which is about 6pa, and the pressure at the inlet is about 1pa, and the pressure at the outlet is about 3pa. Therefore, it is highly possible that the leakage may occur on the contact surface of the two blocks. The design option I was abandoned at a certain point of this study.

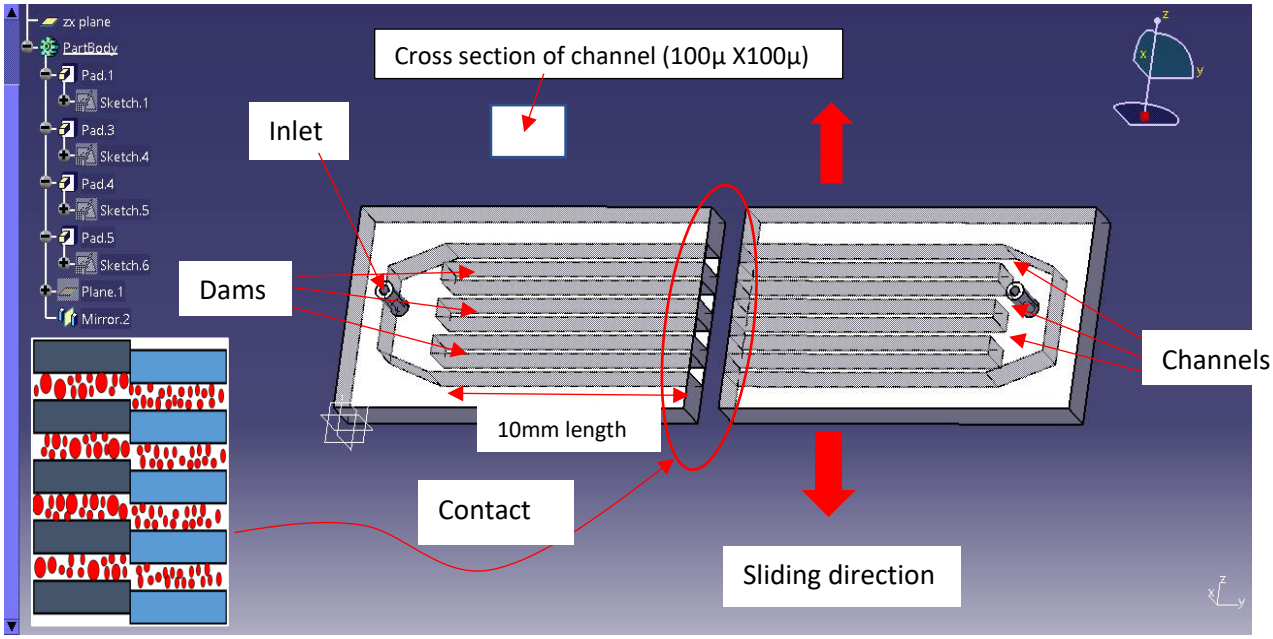

Fig. 3.1 The embodiment design for design option I.

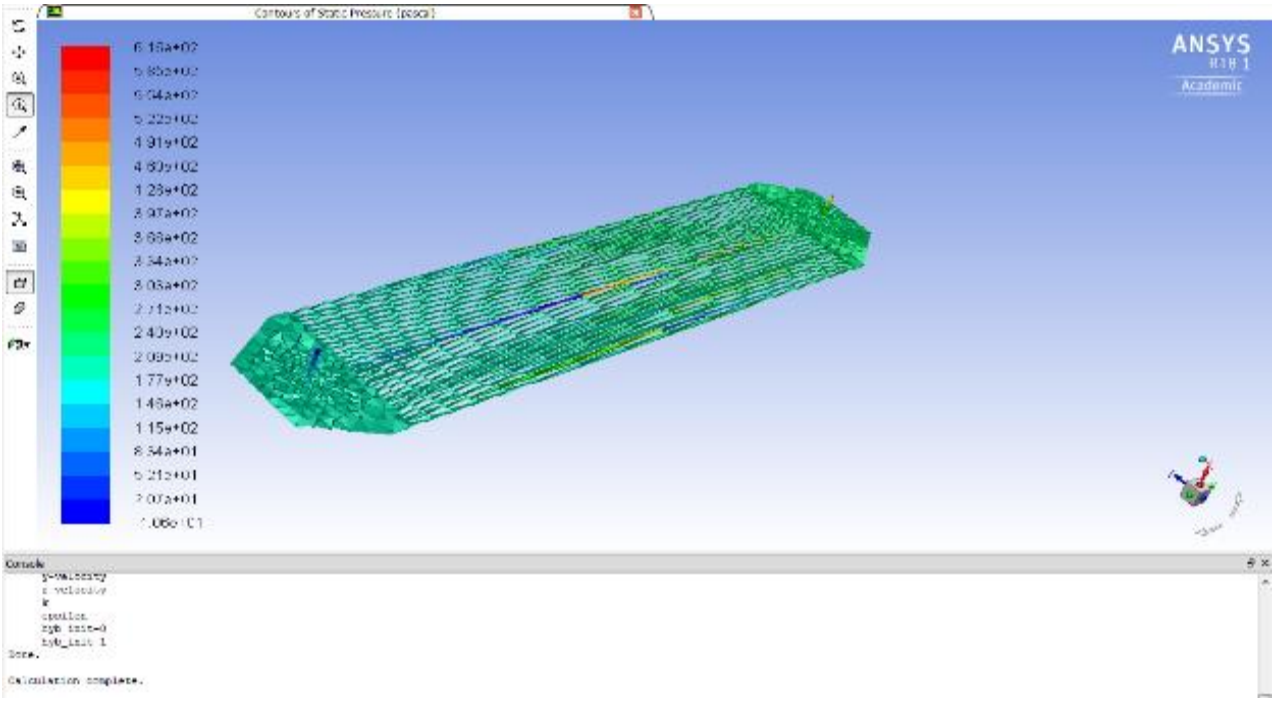

Fig. 3.2 The result of simulation of the pressure in fluid for design option I.

3.4.2 Design option II

Fig. 3.3 shows the embodiment design for the design option II. In this design, there are two sheets (top and bottom). On each sheet, there are a few wells (however, in this thesis only one well is considered without loss of generality), which are in the form of a square. Specifically, on the top sheet, the square is convex with a protruded part, and in the bottom sheet, the square is concave. After the two sheets are assembled (the top on the bottom), they form a system as shown in Fig. 3.4. Fig. 3.5 shows the mechanism, which consists of the guide, rack, the top block and bottom block. The top and bottom sheets in Fig. 3.3 are embedded in the top and bottom blocks,

respectively, and the top block will be further driven by a single axial stage (which has the motion resolution of ~3 um) to be discussed in the experiment in Chapter 5. The material of the sheets in Fig. 3.3 is PDMS, as they will directly contact cells and PDMS is a commonly used material for interacting with cells. The material of the driving mechanism in Fig. 3.5 is full cure 835 Vero white plus.

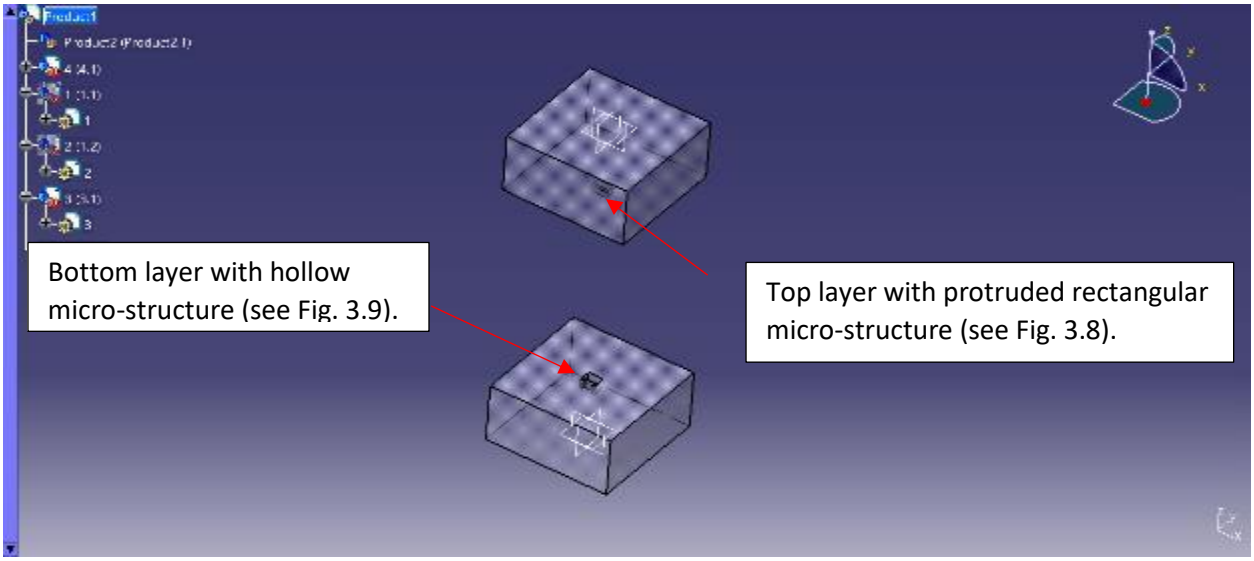

Fig. 3.3 The embodiment design for the design option II.

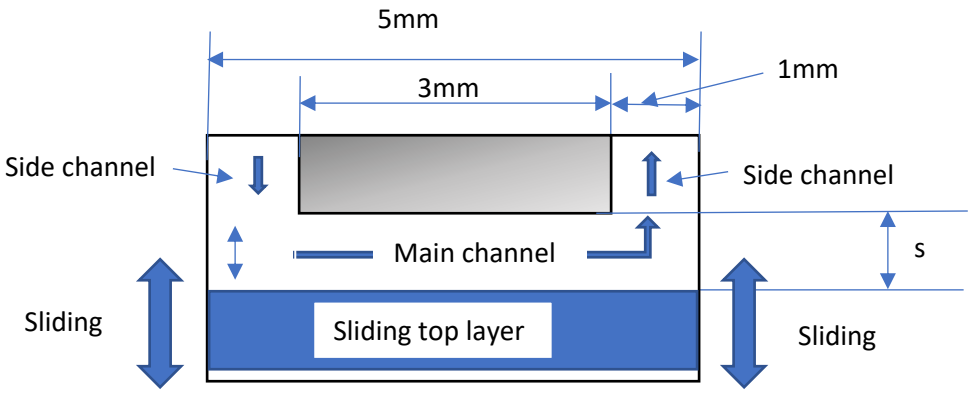

Fig. 3.4 Top view of the device where s changes from 0 to 1 mm.

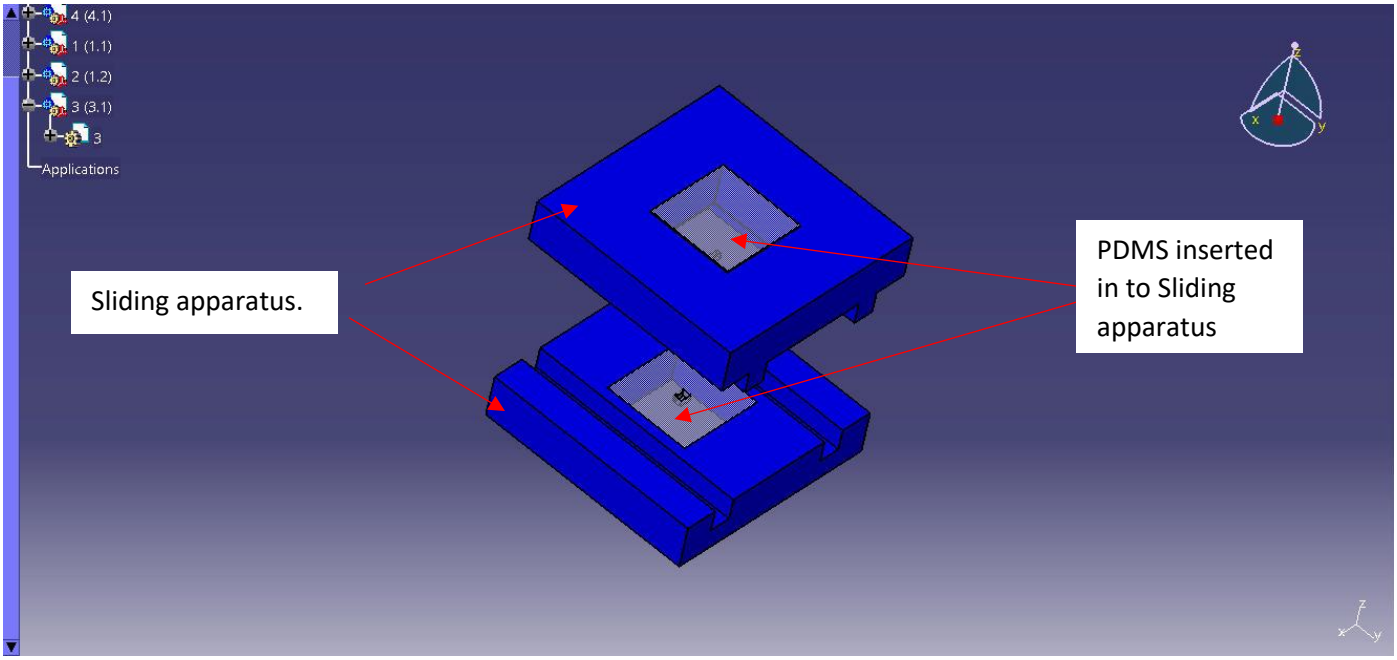

Fig. 3.5 The driving mechanism for the top block.

Let E-DP1: the bottom PDMS sheet; E-DP2: the top PDMS sheet; E-DP3: the bottom Vero white block; E-DP4: the top Vero white block. The above embodiment design, as shown in Fig. 3.3 and Fig. 3.5, embraces the concept design (DP1, DP2b, DP3). The assembly process of these components is as follows: (1) E-DP1 is assembled with E-DP3 into E-(DP1&DP3); (2) E-DP2 is assembled with E-DP4 into E-(DP2&DP4); (3) E-(DP1&DP3), E-(DP2&DP4) assembled to form a whole device. It can be verified that the whole system fulfills all the FRs and CRs. However, satisfying CR 5 is indirectly verified in the sense that the device here is close to the one of Chang et al. (2015) in terms of the force interaction of the device with cells, while they verified that the stress of cells does not damage cells.

3.5 Conclusion

In this chapter, a complete design process for the device was presented, which is expected to fulfill the overall function — to capture single cells of the size range from 2 to 1000 μm with the resolution of 2-5 μm. The design process was based on the design phase theory and axiomatic design theory, and the design axiom called “divide-and-conquer” (Zhang, 2017) was also employed, i.e., the requirement was decomposed into sub-requirements, three sub-requirements in this case. The concept design process resulted in two concept design options. The embodiment process showed one concept design option was difficult to make and thus abandoned. Finally, it comes with one complete design, which meets the requirement. The next chapter will present how the device option II is fabricated.

CHAPTER 4

FABRICATION AND ASSEMBLY

4.1 Introduction

This chapter presents the detailed information of the fabrication process of the device presented in Chapter 3. The fabrication applied the soft lithography technology. There is a discussion of the pros and cons of different soft lithography processes employed in this thesis. The fabrication also includes the assembly of all components along with the test apparatus. Section 4.2 gives a background to the soft lithography technology. Section 4.3 presents the process of fabrication of all the components as described in Chapter 3, embodiment design option II in this case (see Chapter 3). Section 4.4 describes the assembly process. Finally, there is a conclusion in Section 4.5.

4.2 Soft Lithography

According to (Xia and Whitesides, 1998), the soft lithography technology refers to a set of non-photolithography technology, which can make the features of a device from 30 nm to 100 μm. There are several methods with the soft lithography technology, but all of them are related to one same feature – that is, polymer-based products made from the molds that can be in a concave or convex shape. In this thesis, two techniques were employed to make the microfluidic

device, namely replica molding and 3D printing. To further make a closure channel in the device, the bonding operation needs to be applied.

4.2.1 Replica Molding

Replica molding is an effective way for duplication of complex three-dimensional nanometer structures on a soft polymer like PDMS. Masters (mold) are produced by different techniques such as etching in silicon, electroforming metal, and photolithography. Fig. 4.1 illustrates the photolithography process to make a mold for further making a PDMS mold, where the photoresist and substrate together become a mold (convex mold), which is used as a mold for making the PDMS mold. It is noted that SU-8 is a photoresist that enjoys its advantage of high aspect ratio and mechanical and chemical stability with excellent coating.

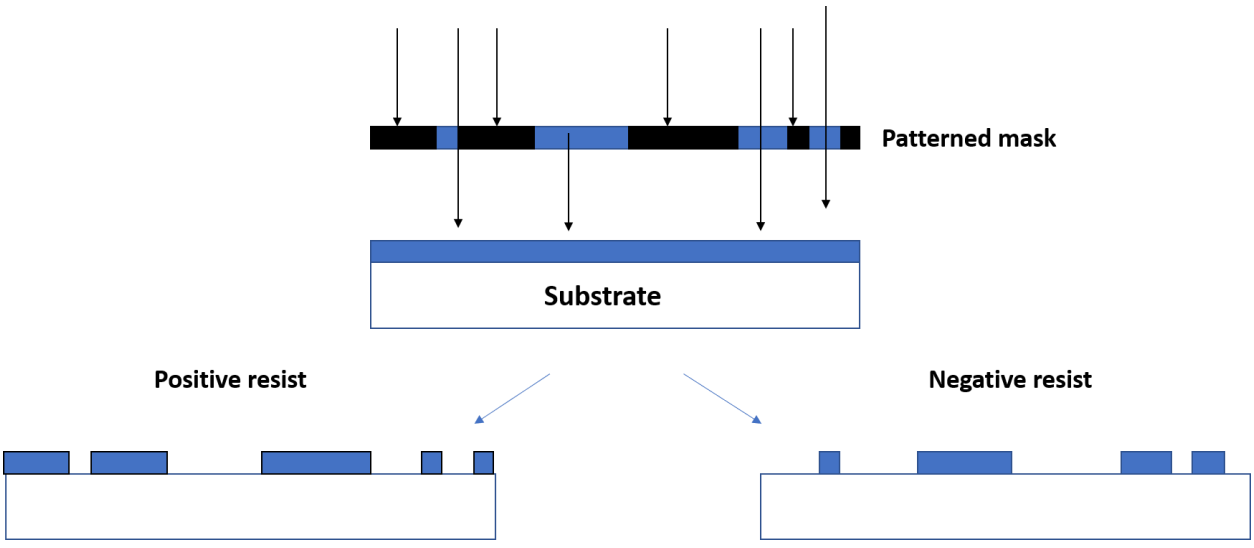

Fig. 4.1 Fabrication process involving positive resist and negative resist to create mold.

It is noted that the replica molding has an advantage of making PDMS channels, as the interaction of PDMS with SU-8 is very little, so the surface finish quality of the PDMS channels is much guaranteed. In this study, the fabrication of the design option I was planned by using the replica molding with SU-8 and Si-substrate as a mold for PDMS. However, as discussed in Chapter 3, the design option I was denied after a careful analysis of the feasibility of assembly.

4.2.2 3D printed Molding

The 3D printing is a nickname for additive manufacturing or rapid prototyping. The basic principle of 3D printing technology is to build a part layer-by-layer. There are several methods with 3D printing, and Polyjet is one of them. The polyjet works in a similar way as the inkjet with the difference being that the former drops the melt, which is further cured by UV light, while the latter drops molten melt on a board which has a lower temperature than the molten melt, and then the molten melt solidifies on the cold board. In Polyjet, the role of UV light is to harden the melt. One salient feature with Polyjet is that it can deposit multiple materials at the same time. Another salient feature with Polyjet is that a wide range of materials can be deposited. Another salient feature with Polyjet is that it can fabricate the part with an overall size greater than 100 µm, which is the case of the design option II. However, the accuracy of Polyjet may be a problem, which was unfortunately the case in this study. Nevertheless, in this study, Polyjet was employed to make a mold for making PDMS parts, as it may be meaningful to the proof-of-concept and experience gaining.

4.3 The fabrication Process for Design Option II

4.3.1 Mold making

The mold was made by a 3D printing technology, Polyjet (EDEN500V) in this case, because the dimension of the device is larger than 100 µm, which excludes the possibility to use photolithography (Fig. 4.1). The material used is Full cure835 Vero white plus because of its rigid and durable properties to obtain high accuracy smaller parts with complex features. The Polyjet machine is available at the Engineering Workshop at the College of Engineering at the University of Saskatchewan. The result of the 3D printed mold is shown in Fig. 4.2. In fact, the top block and bottom block of the sliding mechanism in Fig. 3.5 were also made with this 3D printing machine (Fig. 4.2).

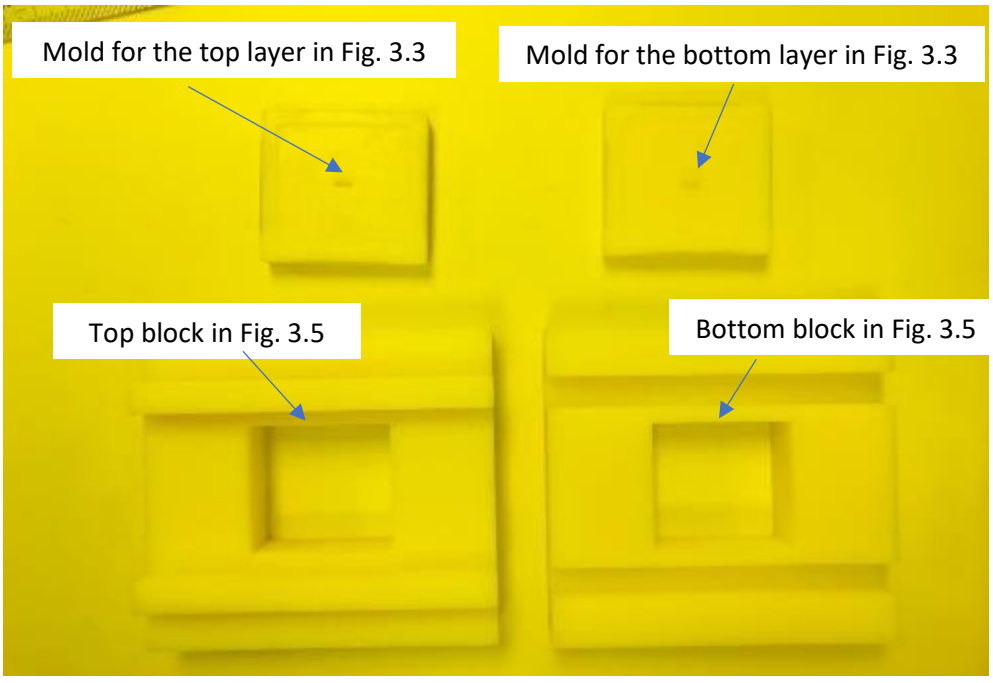

Fig. 4.2 The 3D printed mold and sliding assembly for PDMS (Engineering workshop).

4.3.2 Top and bottom PDMS sheets making

- Step 1: Prebaked the molds in the oven of 85°c for 4 hours to avoid any interaction of unwanted particle present on the surface of the mold during manufacturing.
- Step 2: Did salinization of the mold with 1H,1H,2H,2H-per fluorooctyltricholrosilane (78560-45-9, Alfa Aesar, Ward Hill, MA) in a desiccator for 1 hour at room temperature to prevent any undesired bonding between PDMS (Marrian & Snow, 1996) and the molds, as shown in Fig. 4.3.

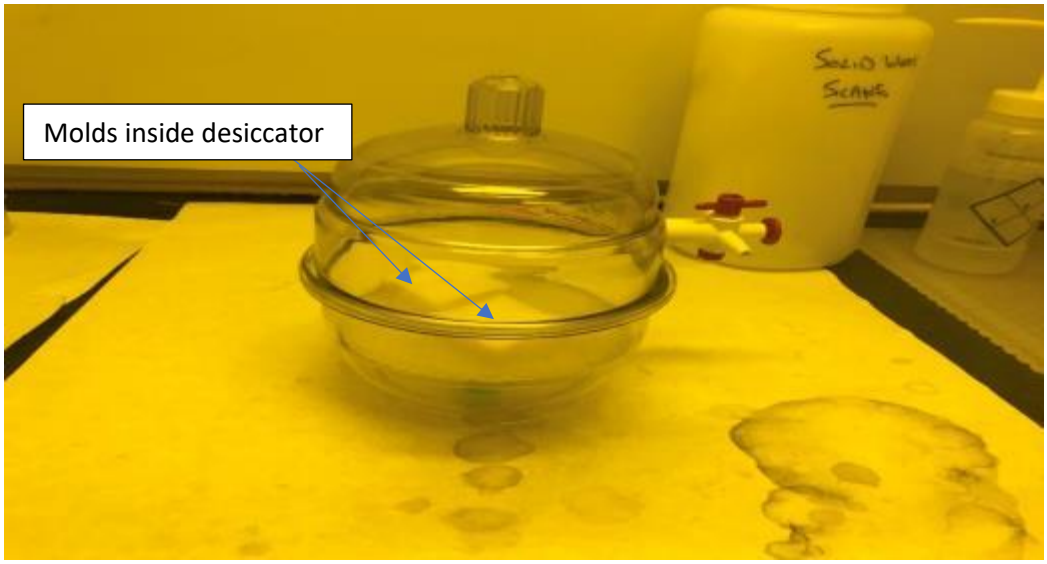

Fig. 4.3 Silanization of the molds (SyLMAND Canadian Light Source).

- Step 3: Prepared the PDMS elastomer and curing agent for the ration of 10:1 (Marrian & Snow, 1996) and then stirred them up using a motorized mixture, as shown in Fig. 4.4.

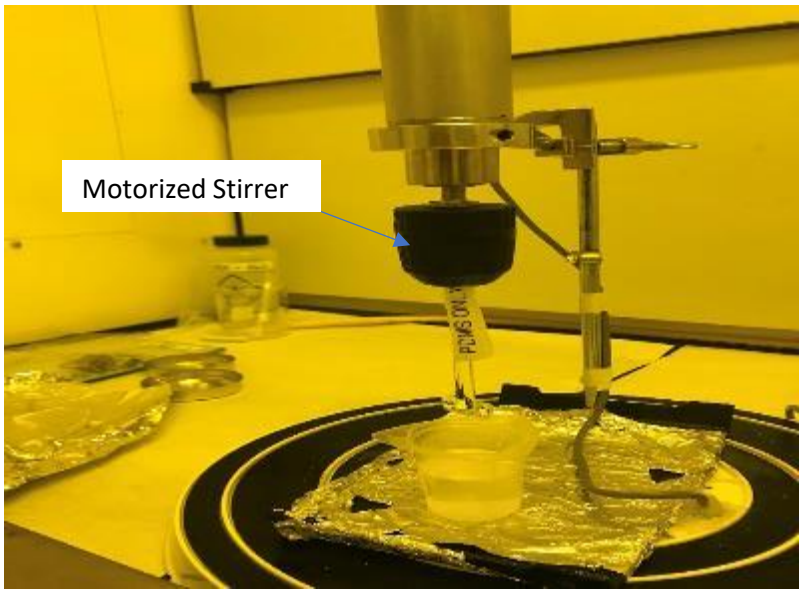

Fig. 4.4 Motorized device to stir mixing agent and curing agent (SyLMAND).

- Step 4: After the proper mixing of PDMS with curing agent, kept PDMS in the vacuum for degassing for one hour to remove air bubbles created in Step 2 while stirring (Fig. 4.5).
- Step 5: After the complete removal of air bubbles, poured PDMS into the mold and kept them in the oven of 65°C for 4 hours, as shown in Fig. 4.5.

Fig. 4.5 Oven and Vacuum chamber (SyLMAND Canadian Light Source).

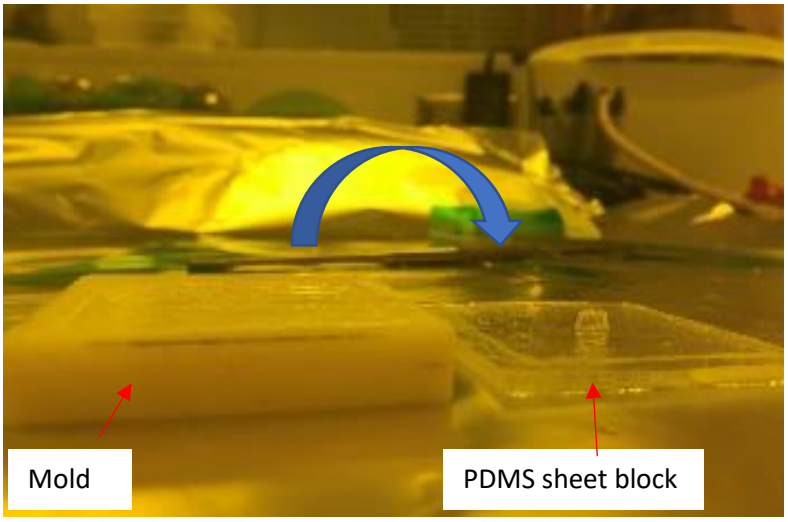

Fig. 4.6 PDMS peeled off from the mold (SyLMAND Canadian Light Source).

- Step 6: Once the completion of solidification, peeled off the PDMS from the mold, as shown in Fig. 4.6 and cleaned the mold with IPA (isopropyl-alcohol) for the next use.

4.4 Assembly

The top and bottom PDMS sheets were assemblied with their corresponding top block and bottom block of the sliding mecahnism with the alignment accuracy of ~0.3 (see Fig. 4.7). The assembly was manually performed under microscope.

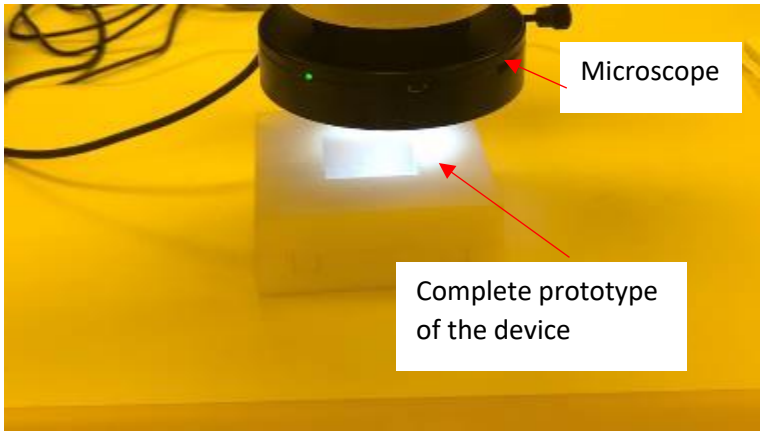

Fig. 4.7 Assembled top and bottom layer of PDMS (SyLMAND Canadian Light Source).

4.5 Conclusion

In this chapter, manufacturing of both design options was discussed with a great detail being put on Design Option II. One lesson learned from the manufacturing of Design Option II is that the peel-off operation of PDMS from the Full cure835 Vero white plus mold is difficult. The future effort should be taken to find a new material for making the mold. Another lesson is that the well size is too large for employing the photolithograph method with SU-8 as photoresist to make the model for making the PDMS part, which could avoid the difficulty of peeling off the PDMS from the mold.

CHAPTER 5

TESTING AND MEASUREMENTS

5.1 Introduction

In this chapter, testing of the device (design option II) is described. The testing includes two parts: measurement of the device to examine whether it meets the design specification in the geometry and topology of the device, and the measurement of the sliding operation to examine the change of the well. All the tests took place at the SyLMAND (Synchrotron Laboratory for Micro and Nano devices). Section 5.2 describes the set-up of the microscope along with its calibration to measure the length. Section 5.3 describes the measurement of the membrane (PDMS sheet). Section 5.4 describes the set-up of the test apparatus to measure the sliding operation. Section 5.5 presents the result of the measurement of the sliding operation. Finally, Section 5.6 is a conclusion.

5.2 Microscope and its Calibration

The microscope Zeiss discovery V8 stereo was used to measure the geometry of the membrane manufactured. The principle of the measurement with the microscope is based on the counting of the imaging pixel. The first step is therefore to calibrate the pixel, i.e., the relation between the pixel and the length. The microscope has a software system called µscope (PixeLINK), which processes the image. The camera and eye piece of the microscope were adjusted with a typical

magnification from 5x to 10x. The focusing knob was set to 1, 6 positions to obtain a clear view of the target object, the device fabricated in this case. As shown in Fig. 5.1, it is observed that 1 mm of the scale was equivalent to 117 pixels. Therefore, the length the one pixel corresponds to was obtained, i.e.:

$$1 \text{ pixel} = \frac{1000\ \mu m}{117} \qquad (5.1)$$

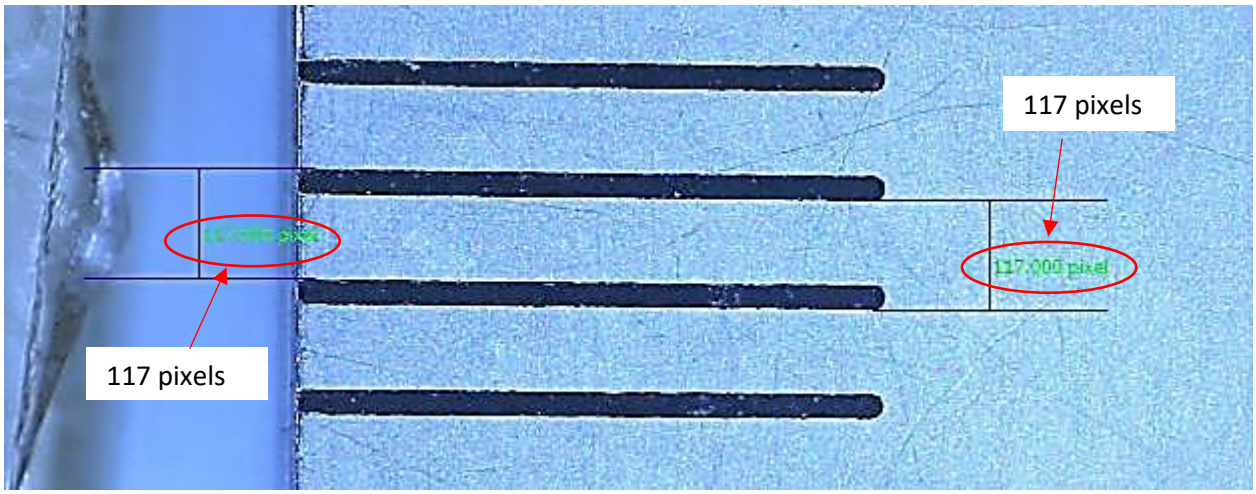

Fig. 5.1 The focused ruling scale under digital microscope.

From Equation (5.1), one pixel is approximately equivalent to 8.547µm. Therefore, the minimum channel space that can be measured using the instrument available is 8.547µm. Fig. 5.2 gives the relation between the pixel and the length (in the range of 1 mm). From Fig. 5.2, it can be seen that the adjustment range of 8.547 µm to 1 mm which corresponds to the pixel from 1 to 117.

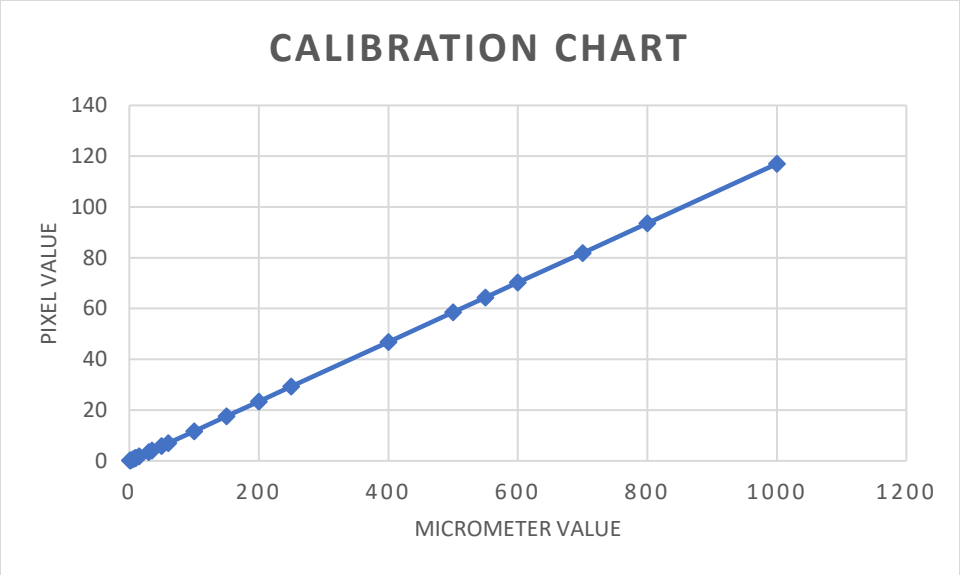

Fig. 5.2 Calibration of the pixel.

5.3 Result of the Measurement of the Geometry of the Device

It is noted that the detailed design of the top PDMS sheet has the following dimensions (Fig. 5.3): the length of 4.9 mm (4900 µm), the width of 2 mm (2000 µm), and the thickness of 3 mm (3000 µm). The measurement of the fabricated PDMS top sheet results in (Fig. 5.4): the length of 585 pixels, the width of 234 pixels, which correspond to the length of 4999.95 µm (~4.9 mm) and the width of 1999.98 µm (~1.9 mm). The result is quite satisfactory. It was also observed that the PDMS sheet was eroded on the sides (Fig. 5.4), which reduces the accuracy of the channel spacing. In Fig. 5.4, the length is further translated to be about 5 mm (5000µm) and the width is translated to be about 3 mm (3000µm). This happened because the PDMS has some stickiness with the mold during the curing process, so the peeling process was not clean.

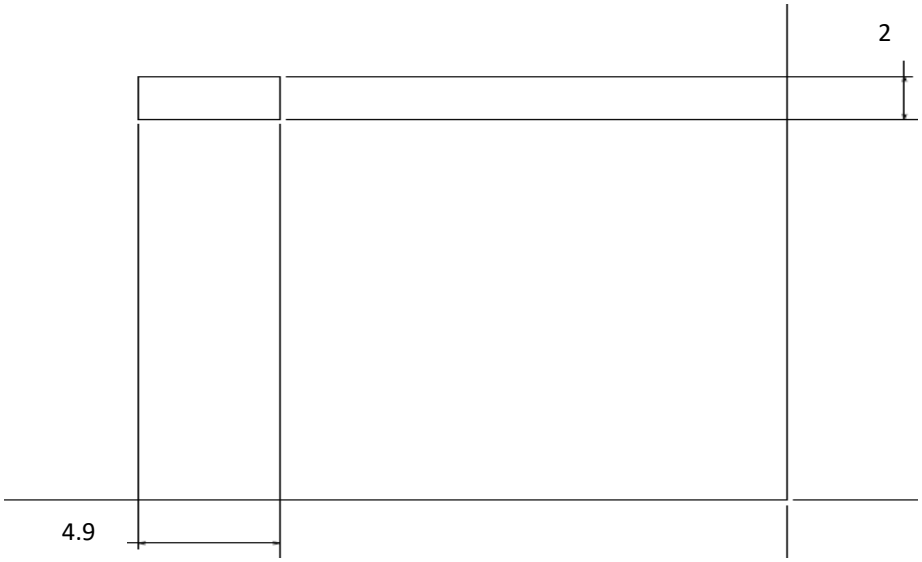

Fig. 5.3 Detailed view of the top sheet with the rectangular microstructure.

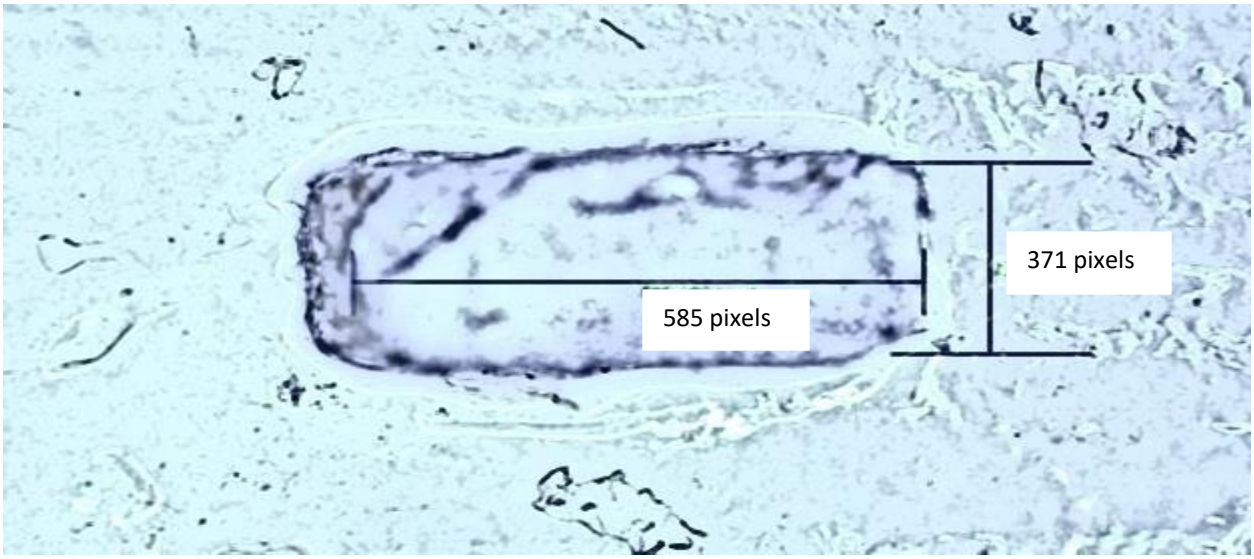

Fig. 5.4 Measurements of the captured top sheet (E-DP2) in the digital microscope.

To the bottom PDMS sheet, the detailed design is shown in Fig. 5.5 with the width of 5 mm, the length of 4 mm, and the thickness of 3 mm. The measurement on the fabricated PDMS sheet

results in: the length of 585 pixels and the width of 371 pixels, which correspond to the length of 4999.995 µm (5 mm) and the width of 3170.93 µm (~3 mm). Therefore, the fabrication seems to be successful. It was observed that some areas on the surface of the structure were damaged. This was with the same reason as that for the top PDMS sheet.

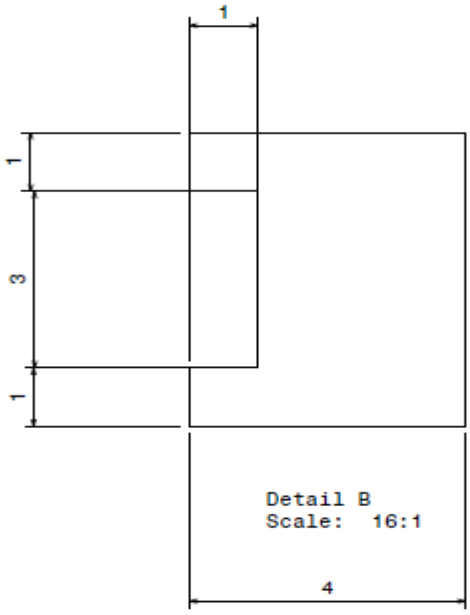

Fig. 5.5 Detailed view of bottom sheet.

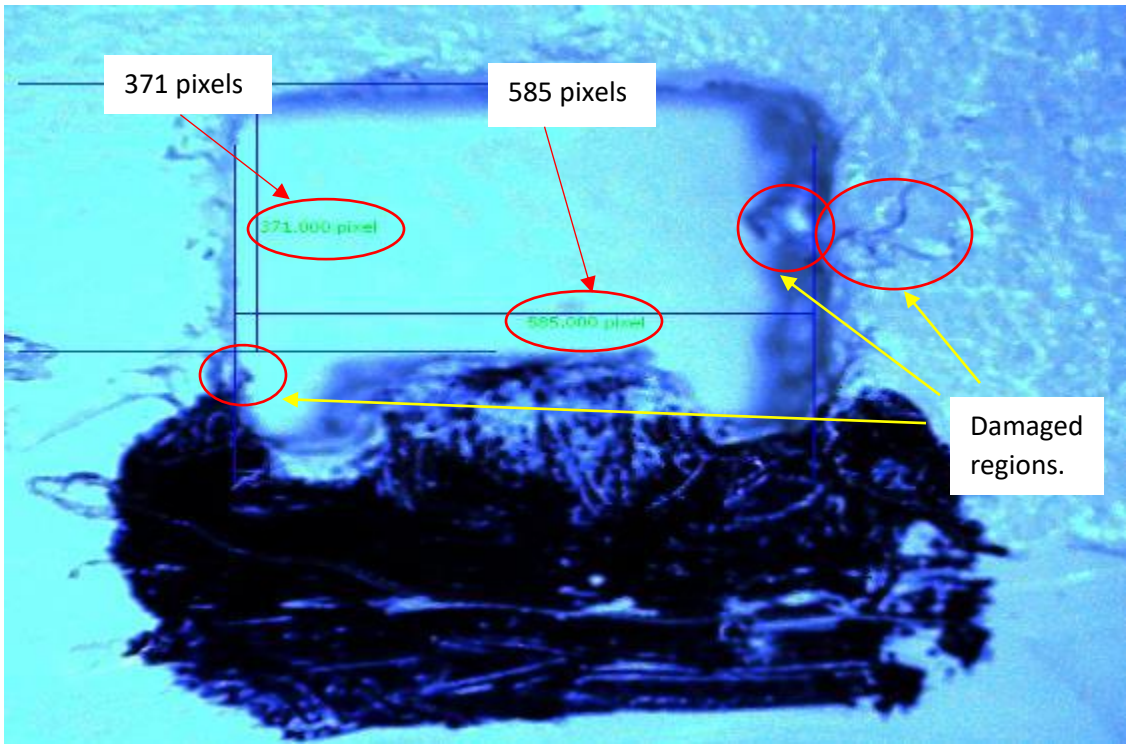

Fig. 5.6 Measurements of the captured bottom sheet (E-DP 1) in the digital microscope.

5.4 Set-up of the Apparatus for the Sliding Operation

The set-up of apparatus for performing the sliding operation is shown in Fig. 5.7, where the whole device (two PDMS sheets and the sliding mechanism) is put on the single-axis motion stage under the microscope. The single-axis motion stage is shown in Fig. 5.8, and it has the resolution of 1 um. In Fig. 5.8, the device was put on the sliding test-bed (Fig. 5.7). By manually turning the screw gauge, the top sheet will slide against the bottom sheet.

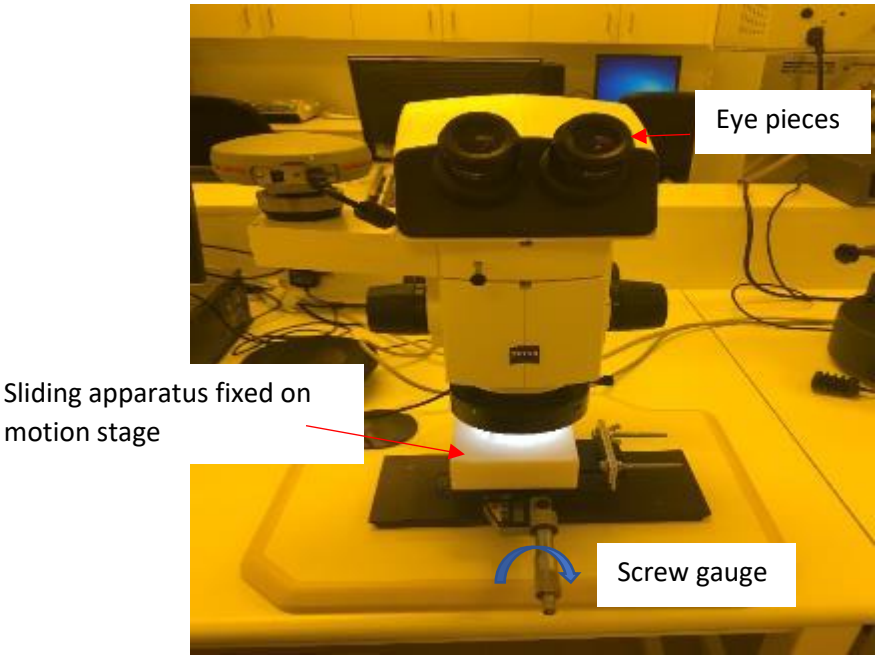

Fig. 5.7 Experimental setup to test channel spacing.

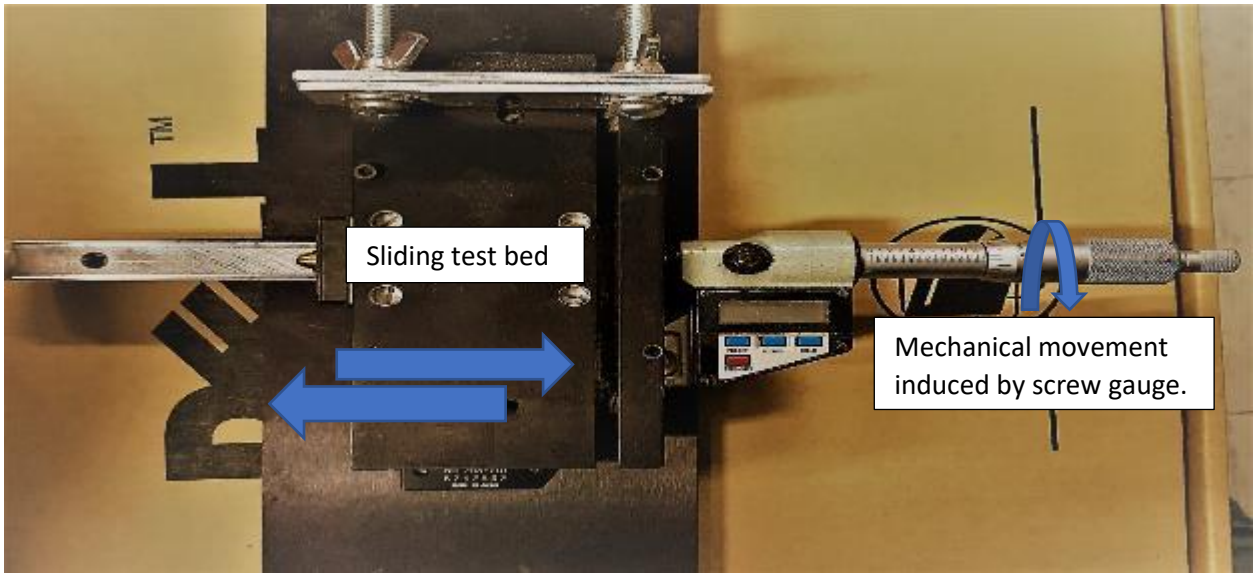

Fig. 5.8 The single axis motion stage used in this work to control channel spacing.

5.5 Results of the Measurement of the Sliding Operation

In the testing process, the first attempt was made to lock the channel spacing (i.e., zero µm) by rotating the screw gauge attached with the motion stage (Fig. 5.8). Fig. 5.9 shows that the device is in a lock status. Then rotating the screw gauge backwards increases the size of the well until the maximum size of the well, as shown in Fig. 5.10. It was observed under the microscope that the maximum channel spacing was 117 pixels, which correspond to 1000 µm nicely. After obtaining the maximum channel spacing and minimum channel spacing, the screw gauge was further adjusted between the maximum spacing and the minimum spacing to verify that the size of the well can be adjusted. Fig. 5.11 shows that the well spacing of 2 pixels (~17.09 µm) (Fig. 5.11A), the well spacing of 6 pixels (~51.28 µm) (Fig. 5.11B), the well spacing of 50 pixels (~427.35 µm) (Fig. 5.11C) and the well spacing of 25 pixels (~213.67 µm) (Fig. 5.11D) were all achieved.

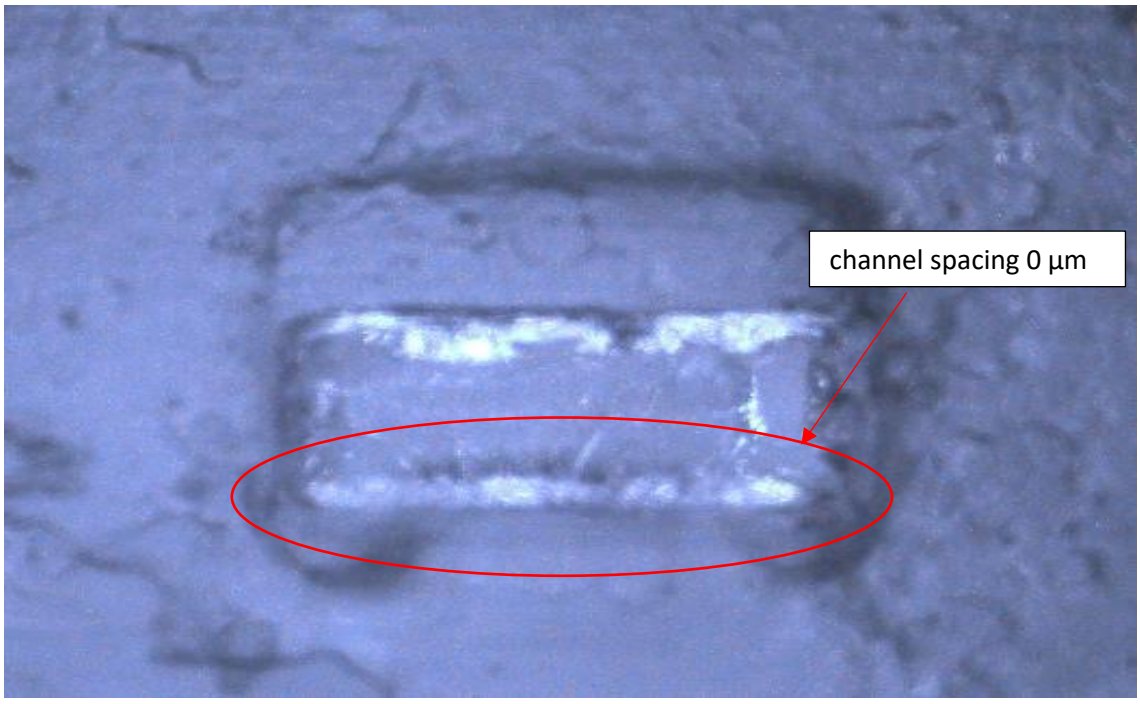

Fig. 5.9 Channel in the locked position.

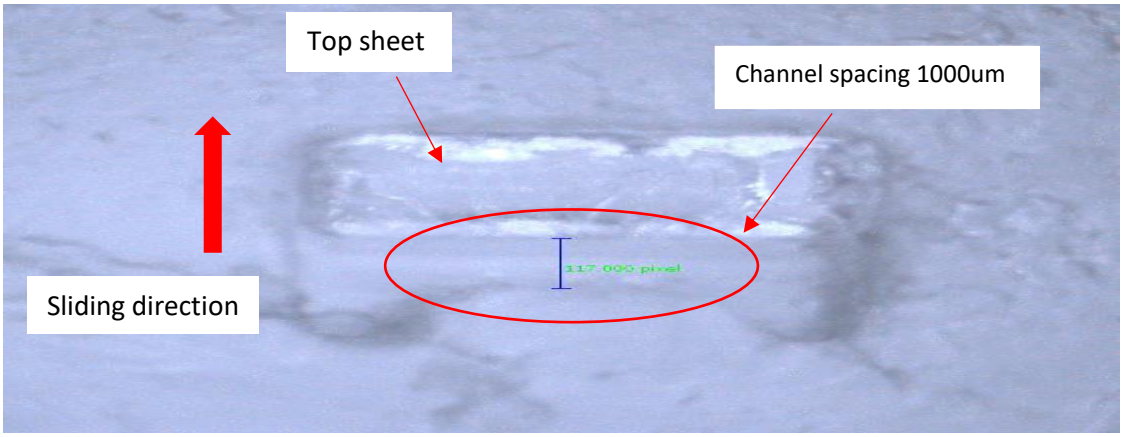

Fig. 5.10 The maximum channel spacing obtained in the new device.

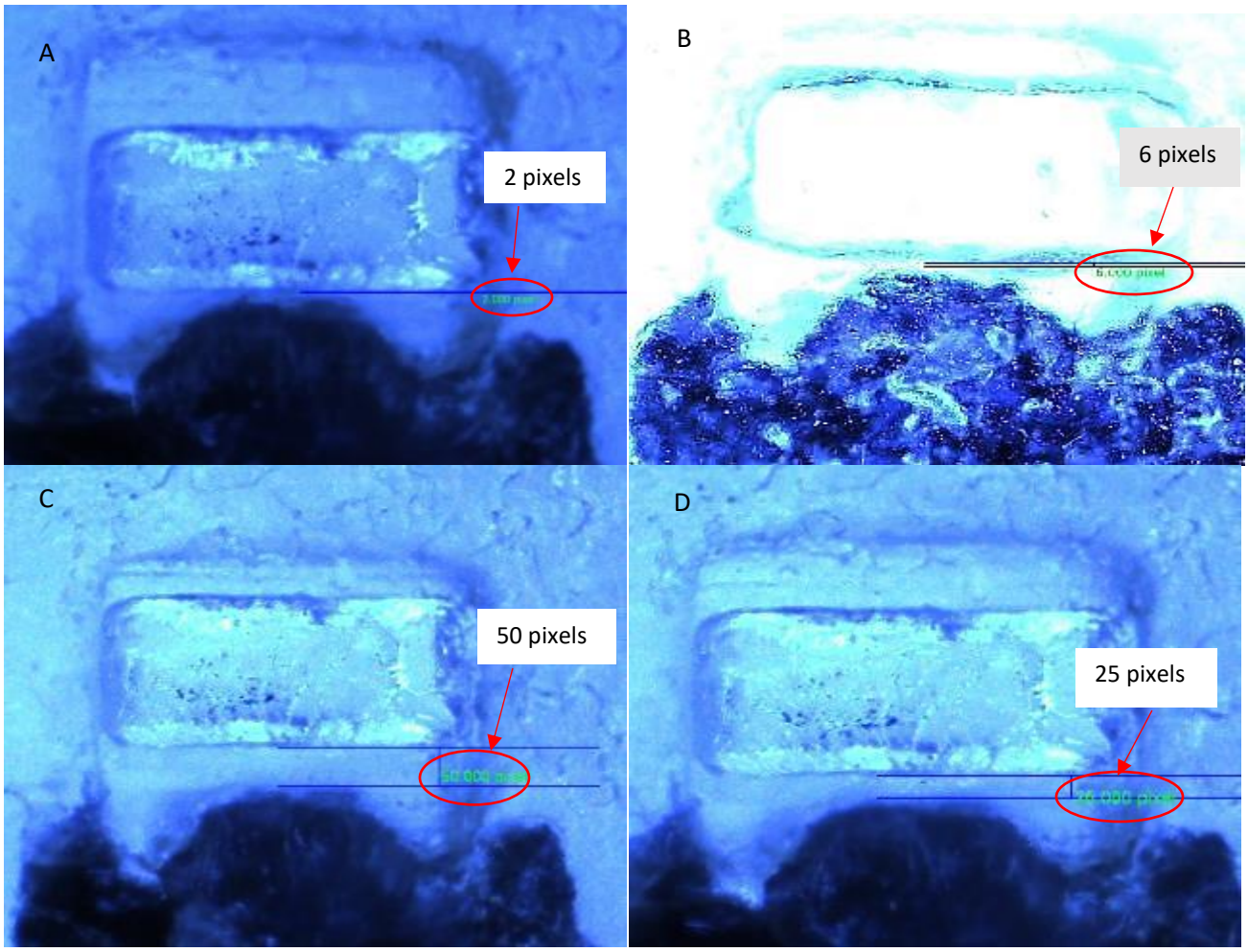

Fig. 5.11 Captured image with different channel spacing (A) with 2pixels, (B) with 6pixels, (C) with 50 pixels, and (D) with 25 pixels.

5.6 Conclusion

In this chapter, the testing of the operation of the whole device was presented, and this included two measurements: measurement of the geometry and shape of the two PDMS sheets and measurement of the sliding operation. The first measurement showed that there was about (~1-2 µm) variation of the fabricated PDMS device with respect to the required device in dimension. The second measurement showed that the device can change the well sizing within the desired range (i.e., 0 to 1000 µm). The smallest change or resolution which can be measured was, however, restricted by the measurement employed in this thesis, which is 8.547 µm. This is not the resolution of the sliding of the device, which was estimated around 3 µm (the resolution of the screw gauge). From the results of the measurements, it can be concluded that the concept of the sliding principle is valid.

CHAPTER 6

CONCULSION AND RECOMMENDATION

6.1 Overview and Conclusions

In the last three decades, numerous microfluidic devices have been developed to ease the clinical diagnostics and biological research. The development of this technology focused on different applications like cell culture and division, separation, morphology, sorting, clone formation and PCR. In particular, to single cells analysis, capturing, positioning and isolation with hydrodynamic concepts, different working principles are available in literature. It is observed that the microfluidic device with mechanical manipulation has some unique advantages when compared to other principles of devices for manipulations of single cells, such as electric, magnetic and acoustic.

However, usually, the device based on the mechanical principle, in fact, other principles as well, cannot deal with the cells of different sizes, and the device is built for the cell of a particular size. This situation results in a waste of energy, time and resources, because every time a new device is required to work with cells of different sizes. Therefore, a new idea arose by investigating the possibility of developing an adjustable microfluidic device which can modify its geometrical features to work with cells of different sizes.

This thesis proposed a new working principle of mechanical manipulation for devices to enable to capture single cells of different sizes, specifically, the size of cells ranging from 0 to 1000 μm with the size resolution of 2 to 5 μm (see the research objectives presented in Chapter 1). It is also the objective to explore the limit of this device technology.

The research first conducted a literature review on various principles and then developed a prototype of the device based on the sliding principle. An experiment to testing whether the size of the well trapper can be varied was carried out on the device as developed. The study (literature study and the experiment) can draw the following conclusions:

(1) The mechanical principle is the best among other principles in terms of the less intrusiveness to cells.
(2) The sliding principle for devices to change the size of the well trapper from 0 to 1000 microns is possible. According to the previous work in our group, which successfully tested cells on an adjustable device (with the deformation principle), there is a high chance for the device built upon the sliding principle to work on cells.

6.2 Contributions

In the field of capturing single cells of different sizes, this thesis advanced the sliding principle of changing the channel spacing or well sizing. In literature, the closed one is called Slip Chip, which was first developed by Rustem F. Ismagilov (http://ismagilovlab.caltech.edu/). The concept of Slip Chip is to change the topology and geometry of a micro-fluidic chip in an off-line manner.

However, this concept was used for changing the connectivity of channels only. The prototype of the device developed in this thesis demonstrated the possibility of changing the size of the well both off-line and on-line in microns. Apparently, the prototype also demonstrates the possibility of changing the topology and geometry of channels both off-line and on-line.

In the field of soft lithography, this thesis was the first try to use the soft material Full cure835 Vero white plus to make a mold by 3D printing for PDMS parts with a good accuracy (~2 μm). This is significant because first, it is very easy and cost effective to 3D print Full cure835 Vero white plus, and second, PDMS is widely used in building micro-fluidic devices.

6.3 Limitations

This work has several limitations. The first limitation is that PDMS reacted with the surface of the 3D printed mold. In the experiment, in the first few attempts, the PDMS did not solidify properly, and the PDMS sheet (molded part) was stick to the mold and damaged during the peel-off process. To address this problem, the 3D printed mold was prebaked in the oven for 85°C for 4 hrs and subsequent curing of PDMS sheet was performed. However, the problem has not completely gone away. This problem is responsible for inaccuracy (~2um) of the molded part in terms of dimension as well as surface damage. That resolution is partially due to the size of the channel, which is 1 mm. The size of the channel affects the focus of the microscopy, and subsequently the number of pixels that can be covered by the view, and thus the resolution in

particular the length per pixel (8.547um now). Suppose that the maximal channel size is 100 μm. Then the measurement resolution will be 0.855 um.

6.4 Future works

Several further works that may overcome the limitations and advance the micro-fluidic device technology are recommended.

First, optimizing the way of making PDMS channels is warranted. In this thesis, a 3D printed mold (thermoplastic) was used to fabricate the PDMS sheets. As pointed out before, this fabrication technique did not achieve what was desired; particularly, there was an unwanted interaction between PDMS and the material used to 3D print the mold. Research is warranted to advance the fabrication technology in two directions. First, additional processes may need to be performed on the internal surface of the mold which is made of the material Full cure835 Vero white plus reduce any possible interaction between PDMS and the mold material. Second, PMMA is suggested as a mold material to avoid the interaction between PDMS and mold. Another future work is directly to print PDMS channel (Bhattacharjee et al., 2016).

Second, the design option II needs to be further modified. Currently, there is a problem of redundancy sliding contact in the device. The first sliding is between the top PDMS sheet and the bottom PDMS sheet. The second sliding is between the top block and bottom block of the sliding mechanism. This duplicated sliding structure violates Axiom 1 or is a conflicting redundant design.

The new design should just let two PDMS sheets slide relative to each other, i.e., one pair of contacts only.

Third, testing of the device on cells is warranted. This is highly possible if the device is completely cured without any contamination, based on the previous work in our group, which is an adjustable well trapper based on the deformation principle. It is noted that the device based on the deformation principle suffers from a small range of adjusting.

Finally, design and fabrication of an array of wells is warranted, which makes the device for a practical use.

LIST OF REFERENCES

Anderson, J. R., Chiu, D. T., Jackman, R. J., Chemiavskaya, O., McDonald, J. C., Wu, H., … Whitesides, G. M. (2000). Fabrication of topologically complex three-dimensional microfluidic systems in PDMS by rapid prototyping. *Analytical Chemistry*, *72*(14), 3158–3164. https://doi.org/10.1021/ac9912294

Beech, J. P., & Tegenfeldt, J. O. (2008). Tuneable separation in elastomeric microfluidics devices. *Lab on a Chip*, *8*(5), 657–659. https://doi.org/10.1039/b719449h

Bhattacharjee, N., Urrios, A., Kang, S., & Folch, A. (2016). The upcoming 3D-printing revolution in microfluidics. *Lab on a Chip*, *16*(10), 1720–1742. https://doi.org/10.1039/c6lc00163g

Brose, S., Danylyuk, S., Juschkin, L., Dittberner, C., Bergmann, K., Moers, J., … Grützmacher, D. (2012). Broadband transmission masks, gratings and filters for extreme ultraviolet and soft X-ray lithography. *Thin Solid Films*, *520*(15), 5080–5085. https://doi.org/10.1016/j.tsf.2012.03.036

Chang, C. W., Peng, C. C., Liao, W. H., & Tung, Y. C. (2015). Polydimethylsiloxane SlipChip for mammalian cell culture applications. *Analyst*, *140*(21), 7355–7365. https://doi.org/10.1039/c5an00547g

Chu, M., Nguyen, T. T., Lee, E. K., Morival, J. L., & Khine, M. (2017). Plasma free reversible and irreversible microfluidic bonding. *Lab Chip*, *17*(2), 267–273. https://doi.org/10.1039/C6LC01338D

Del Campo, A., & Greiner, C. (2007). SU-8: A photoresist for high-aspect-ratio and 3D submicron lithography. *Journal of Micromechanics and Microengineering*, *17*(6).

https://doi.org/10.1088/0960-1317/17/6/R01

Di Carlo, D., Aghdam, N., & Lee, L. P. (2006). Single-cell enzyme concentrations, kinetics, and inhibition analysis using high-density hydrodynamic cell isolation arrays. *Analytical Chemistry*, *78*(14), 4925–4930. https://doi.org/10.1021/ac060541s

Dimmeler, S., Haendeler, J., Rippmann, V., Nehls, M., & Zeiher, A. M. (1996). Shear stress inhibits apoptosis of human endothelial cells. *FEBS Lett*, *399*(1–2), 71–74. https://doi.org/10.1016/S0014-5793(96)01289-6

Franke, T., Braunmüller, S., Schmid, L., Wixforth, A., & Weitz, D. A. (2010). Surface acoustic wave actuated cell sorting (SAWACS). *Lab on a Chip*, *10*(6), 789. https://doi.org/10.1039/b915522h

Guo, P., Hall, E. W., Schirhagl, R., Mukaibo, H., Martin, C. R., & Zare, R. N. (2012). Microfluidic capture and release of bacteria in a conical nanopore array. *Lab on a Chip*, *12*(c), 558. https://doi.org/10.1039/c2lc21092d

Han, K. H., & Bruno Frazier, A. (2004). Continuous magnetophoretic separation of blood cells in microdevlce format. *Journal of Applied Physics*, *96*(10), 5797–5802. https://doi.org/10.1063/1.1803628

Herweijer, H., And, W. S., & Visser, J. W. M. (1988). High speed photodamage cell selection using bromodeoxyuridine/Hoechst 33342 photosensitized cell killing. *Cytometry*, *9*(2), 143–149. https://doi.org/10.1002/cyto.990090208

Huang, S.-H., Tan, W.-H., Tseng, F.-G., & Takeuchi, S. (2006). A monolithically three-dimensional flow-focusing device for formation of single/double emulsions in closed/open microfluidic systems. *Journal of Micromechanics and Microengineering*, *16*(11), 2336–2344.

https://doi.org/10.1088/0960-1317/16/11/013

Huebner, A., Bratton, D., Whyte, G., Yang, M., Andrew, J., & Hollfelder, F. (2009). Static microdroplet arrays : a microfluidic device for droplet trapping , incubation and release for enzymatic and cell-based assays †, 692–698. https://doi.org/10.1039/b813709a

Huh, D., Mills, K. L., Zhu, X., Burns, M. A., Thouless, M. D., & Takayama, S. (2007). Tuneable elastomeric nanochannels for nanofluidic manipulation. *Nature Materials*, *6*(6), 424–428. https://doi.org/10.1038/nmat1907

Langeveld, L. (2011). Product Design with Embodiment Design as a New Perspective. *Industrial Design--New Frontiers*, 121. https://doi.org/10.5772/20579

Lawrenz, A., Nason, F., & Cooper-White, J. J. (2012). Geometrical effects in microfluidic-based microarrays for rapid, efficient single-cell capture of mammalian stem cells and plant cells. *Biomicrofluidics*, *6*(2). https://doi.org/10.1063/1.4704521

MacDonald, M. P., Spalding, G. C., & Dholakia, K. (2003). Microfluidic sorting in an optical lattice. *Nature*, *426*(November), 421–424. https://doi.org/10.1038/nature02120.1.

Marrian, C. R. K., & Snow, E. S. (1996). Proximal probe lithography and surface modification. *Microelectronic Engineering*, *32*(1–4 SPEC. ISS.), 173–189. https://doi.org/10.1016/0167-9317(96)00005-6

Mcdonald, J. C., Duffy, D. C., Anderson, J. R., & Chiu, D. T. (2000). Review General Fabrication of microfluidic systems in poly (dimethylsiloxane).

Melngailis, J. (1993). Focused ion beam lithography. *Nuclear Instruments and Methods in Physics Research Section B: Beam Interactions with Materials and Atoms*, *80–81*, 1271–1280. https://doi.org/10.1016/0168-583X(93)90781-Z

Moolman, M. C., Huang, Z., Krishnan, S. T., Kerssemakers, J. W. J., & Dekker, N. H. (2013). Electron beam fabrication of a microfluidic device for studying submicron-scale bacteria. *Journal of Nanobiotechnology*, *11*, 12. https://doi.org/10.1186/1477-3155-11-12

Murray, C., McCoul, D., Sollier, E., Ruggiero, T., Niu, X., Pei, Q., & Carlo, D. Di. (2013). Electro-adaptive microfluidics for active tuning of channel geometry using polymer actuators. *Microfluidics and Nanofluidics*, *14*(1–2), 345–358. https://doi.org/10.1007/s10404-012-1055-y

O'Sullivan, G., Kilbane, D., & Darcy, R. (2012). Recent progress in source development for extreme UV lithography. *Journal of Modern Optics*, *59*(10), 855–872. https://doi.org/10.1080/09500340.2012.678399

Palatnikov, M. N., Kokhanchik, L. S., Emelin, E. V., Sidorov, N. V., & Manukovskaya, D. V. (2016). Creation of domains by direct electron beam writing in magnesium-doped LiNbO3and LiNbO3:Fe single crystals. *Nuclear Instruments and Methods in Physics Research, Section B: Beam Interactions with Materials and Atoms*, *370*, 107–113. https://doi.org/10.1016/j.nimb.2016.01.026

Rettig, J. R., & Folch, A. (2005). Large-scale single-cell trapping and imaging using microwell arrays. *Analytical Chemistry*, *77*(17), 5628–5634. https://doi.org/10.1021/ac0505977

Schut, T. C. B., Grooth, B. G. De, & Greve, J. (1990). A New Principle of Cell Sorting by Using Selective Electroporation in a Modified Flow Cytometer Vmt, *666*, 659–666.

Soberanes, E. E. M., Soberanes, E. E. M., & All, J. (2016). AN ADAPTABLE SINGLE CELL-TRAPPING DEVICE FOR A WIDE RANGE OF CELL SIZES A Thesis Submitted to the College of Graduate Studies and Research in Partial Fulfillment of the Requirements for the Degree of Master of

Science in the Department of Mechanical Engineering, (June 2016).

Sochol, R. D., Dueck, M. E., Li, S., Lee, L. P., & Lin, L. (2012). Hydrodynamic resettability for a microfluidic particulate-based arraying system. *Lab on a Chip*, *12*(23), 5051–5056. https://doi.org/10.1039/c2lc40704c

Suh, N. P., Cochran, D. S., & Lima, P. C. (1998). Manufacturing system design. *CIRP Annals - Manufacturing Technology*, *47*(2), 627–639. https://doi.org/10.1016/S0007-8506(07)63245-4

Tan, W.-H., & Takeuchi, S. (2007). A trap-and-release integrated microfluidic system for dynamic microarray applications. *Proceedings of the National Academy of Sciences*, *104*(4), 1146–1151. https://doi.org/10.1073/pnas.0606625104

Tice, J. D., Bassett, T. A., Desai, A. V., Apblett, C. A., & Kenis, P. J. A. (2013). A monolithic poly(dimethylsiloxane) electrostatic actuator for controlling integrated pneumatic microsystems. *Sensors and Actuators, A: Physical*, *196*, 22–29. https://doi.org/10.1016/j.sna.2013.03.020

W.J. Zhang, Y. Lin, N. S. (2005). On the Function-Behavior-Structure Model for Design. *Canadian Design Engineering Network Conference 2005*. https://doi.org/10.24908/pceea.v0i0.3884

Whitesides, G. M. (2006). The origins and the future of microfluidics. *Nature*, *442*(7101), 368–373. https://doi.org/10.1038/nature05058

Xia, Y., & Whitesides, G. M. (1998). Soft Lithography. *Angewandte Chemie International Edition*, *37*(5), 550–575. https://doi.org/10.1002/(SICI)1521-3773(19980316)37:5<550::AID-ANIE550>3.0.CO;2-G

Yi, C., Li, C. W., Ji, S., & Yang, M. (2006). Microfluidics technology for manipulation and analysis

of biological cells. *Analytica Chimica Acta*, *560*(1–2), 1–23. https://doi.org/10.1016/j.aca.2005.12.037

Yu, S. cang, Ping, Y. fang, Yi, L., Zhou, Z. hua, Chen, J. hong, Yao, X. hong, … Bian, X. wu. (2008). Isolation and characterization of cancer stem cells from a human glioblastoma cell line U87. *Cancer Letters*, *265*(1), 124–134. https://doi.org/10.1016/j.canlet.2008.02.010

Zheng, S., Lin, H., Liu, J. Q., Balic, M., Datar, R., Cote, R. J., & Tai, Y. C. (2007). Membrane microfilter device for selective capture, electrolysis and genomic analysis of human circulating tumor cells. *Journal of Chromatography A*, *1162*(2 SPEC. ISS.), 154–161. https://doi.org/10.1016/j.chroma.2007.05.064

Zhu, J., Shang, J., Olsen, T., Liu, K., Brenner, D., & Lin, Q. (2014). A mechanically tunable microfluidic cell-trapping device. *Sensors and Actuators, A: Physical*, *215*, 197–203. https://doi.org/10.1016/j.sna.2013.10.016

Zhang, W.J., 2017. Lecture notes (rapid prototyping), ME 330, Department of Mechanical Engineering, University of Saskatchewan.

Appendix A: Permission of reuse content

ELSEVIER LICENSE
TERMS AND CONDITIONS

Oct 24, 2018

This Agreement between University of Saskatchewan--- Annal Arumugam ("You") and Elsevier ("Elsevier") consists of your license details and the terms and conditions provided by Elsevier and Copyright Clearance Center.

License Number	4455560159111
License date	Oct 24, 2018
Licensed Content Publisher	Elsevier
Licensed Content Publication	Analytica Chimica Acta
Licensed Content Title	Microfluidics technology for manipulation and analysis of biological cells
Licensed Content Author	Changqing Yi,Cheuk-Wing Li,Shenglin Ji,Mengsu Yang
Licensed Content Date	Feb 23, 2006
Licensed Content Volume	560
Licensed Content Issue	1-2
Licensed Content Pages	23
Start Page	1
End Page	23
Type of Use	reuse in a thesis/dissertation
Portion	figures/tables/illustrations
Number of figures/tables/illustrations	2
Format	electronic
Are you the author of this Elsevier article?	No
Will you be translating?	Yes, including English rights
Number of languages	1
Languages	English
Original figure numbers	Fig. 1 and Fig. 4
Title of your thesis/dissertation	On the sliding principle of microfluidic device to capture single cells.
Expected completion date	Dec 2018

Estimated size (number of pages)	70
Requestor Location	University of Saskatchewan 105 administration building saskatoon, SK S7N5A2 Canada Attn: Annal Arumugam
Publisher Tax ID	GB 494 6272 12
Total	0.00 USD

SPRINGER NATURE LICENSE TERMS AND CONDITIONS

Oct 24, 2018

This Agreement between University of Saskatchewan--- Annal Arumugam ("You") and Springer Nature ("Springer Nature") consists of your license details and the terms and conditions provided by Springer Nature and Copyright Clearance Center.

License Number	4455590498487
License date	Oct 24, 2018
Licensed Content Publisher	Springer Nature
Licensed Content Publication	Nature Materials
Licensed Content Title	Tuneable elastomeric nanochannels for nanofluidic manipulation
Licensed Content Author	Dongeun Huh, K. L. Mills, Xiaoyue Zhu, Mark A. Burns, M. D. Thouless et al.
Licensed Content Date	May 7, 2007
Licensed Content Volume	6
Licensed Content Issue	6
Type of Use	Thesis/Dissertation
Requestor type	academic/university or research institute
Format	print and electronic
Portion	figures/tables/illustrations
Number of figures/tables/illustrations	1
High-res required	no
Will you be translating?	no
Circulation/distribution	<501
Author of this Springer Nature content	no
Title	On the sliding principle of microfluidic device to capture single cells.
Institution name	university of saskatchewan
Expected presentation date	Dec 2018
Portions	Fig. 1
Requestor Location	University of Saskatchewan 105 administration building saskatoon, SK S7N5A2

	Canada Attn: University of Saskatchewan
Billing Type	Invoice
Billing Address	University of Saskatchewan 105 administration building saskatoon, SK S7N5A2 Canada Attn: Annal Arumugam
Total	0.00 USD

Copyright Clearance Center

Note: Copyright.com supplies permissions but not the copyrighted content itself.

1 PAYMENT 2 REVIEW 3 CONFIRMATION

Step 3: Order Confirmation

Thank you for your order! A confirmation for your order will be sent to your account email address. If you have questions about your order, you can call us 24 hrs/day, M-F at +1.855.239.3415 Toll Free, or write to us at info@copyright.com. This is not an invoice.

Confirmation Number: 11759493
Order Date: 10/24/2018

If you paid by credit card, your order will be finalized and your card will be charged within 24 hours. If you choose to be invoiced, you can change or cancel your order until the invoice is generated.

Payment Information

Annal Arumugam
ana953@mail.usask.ca
+1 (306) 250-9726
Payment Method: n/a

Order Details

Lab on a chip

Order detail ID: 71624786
Order License Id: 4455570818696
ISSN: 1473-0189
Publication Type: e-Journal
Volume:
Issue:
Start page:
Publisher: ROYAL SOCIETY OF CHEMISTRY
Author/Editor: Royal Society of Chemistry (Great Britain)

Permission Status: Granted
Permission type: Republish or display content
Type of use: Thesis/Dissertation
View details

Note: This item will be invoiced or charged separately through CCC's **RightsLink** service. More info **$ 0.00**

Total order items: 1

This is not an invoice.

Order Total: 0.00 USD

Appendix B: FEM modeling and analysis of the design option I

In fluid dynamics, fluid flow is mathematically described using four significant physical quantities, which are flow velocity, flow pressure, fluid density, and fluid viscosity. The objective of flow simulation is to track the fluid velocity and pressure variations at different points in the fluid domain. The flow velocity and flow pressure are different at a different point in a fluid volume. There are many kinds of fluid flow. A flow can be compressible or incompressible, viscous or inviscid, steady or unsteady and laminar or turbulent. The fluid flow concerned by this thesis is laminar flow, and in this simulation, water properties are used to predict the fluid pressure exerted on the micro-channel instead of actual cell carrier fluid which does not have much difference by keeping the velocity of the fluid as constant.

This modeling process divided into four steps, which are Framing fluid domain, Meshing, Boundary condition, and Solution Visualization.

1. In this fluent simulation, channel boundary (depicted in Fig. A.1 with the shaded region) is used as a domain object to pass the fluid inside by subtracting the other solid surface expect the channels with inlet and outlet in the below design. Thus, the fluid domain confined by the surface of the channel structure in contact with the fluid for internal flow. In a scenario only single fluid simulation is possible.

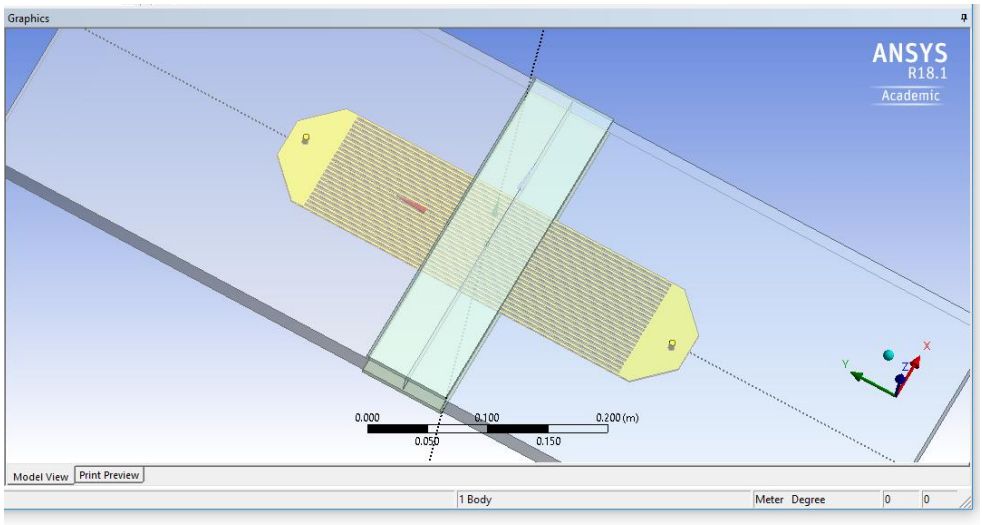

Fig. B.1 Fluid domain framed for the device.

2. A triangular mesh is created as depicted in Fig. A.2 for the fluid domain to predict the accuracy, solution time and rate of convergence. A Mesh value range from -100 to +100 and default value is zero. In this case it is changed to +100 to get slower speed solution, finer mesh and high accuracy.

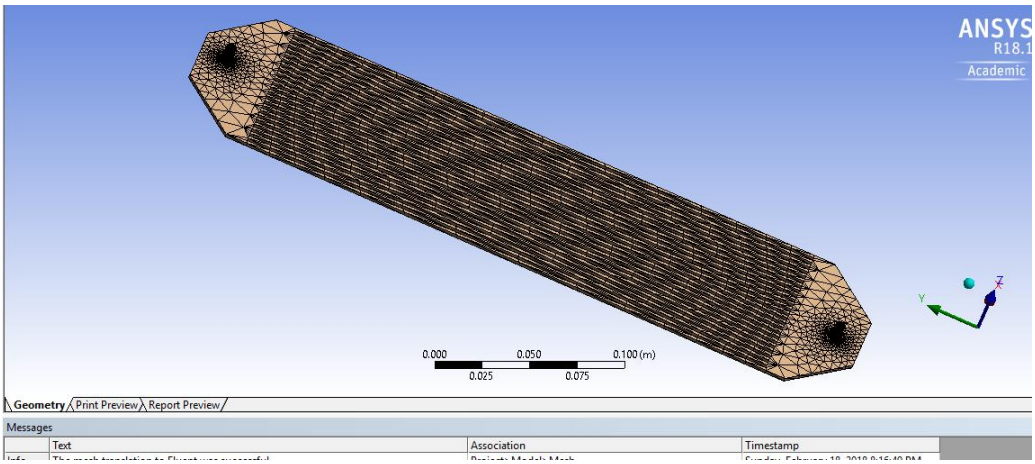

Fig. B.2 Mesh created for the fluid domain.

3. Boundary conditions applied in this simulation is inlet point which is available on the left corner of the device and outlet point which is available on the right corner of the device as illustrated in Fig. A.3 with green points.

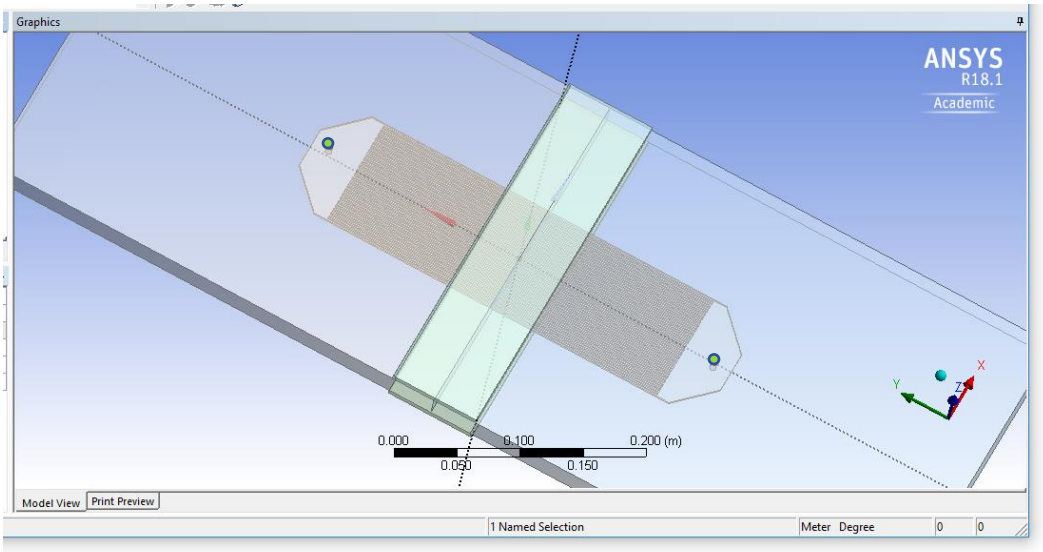

Fig. B.3 Inlet and outlet boundary conditions.

4. Once a problem is setup with the fluid domain meshed and the boundary conditions specified, it can be submitted to the solver for computation of a solution.

Appendix C: Engineering drawings of the detail design for the design option II

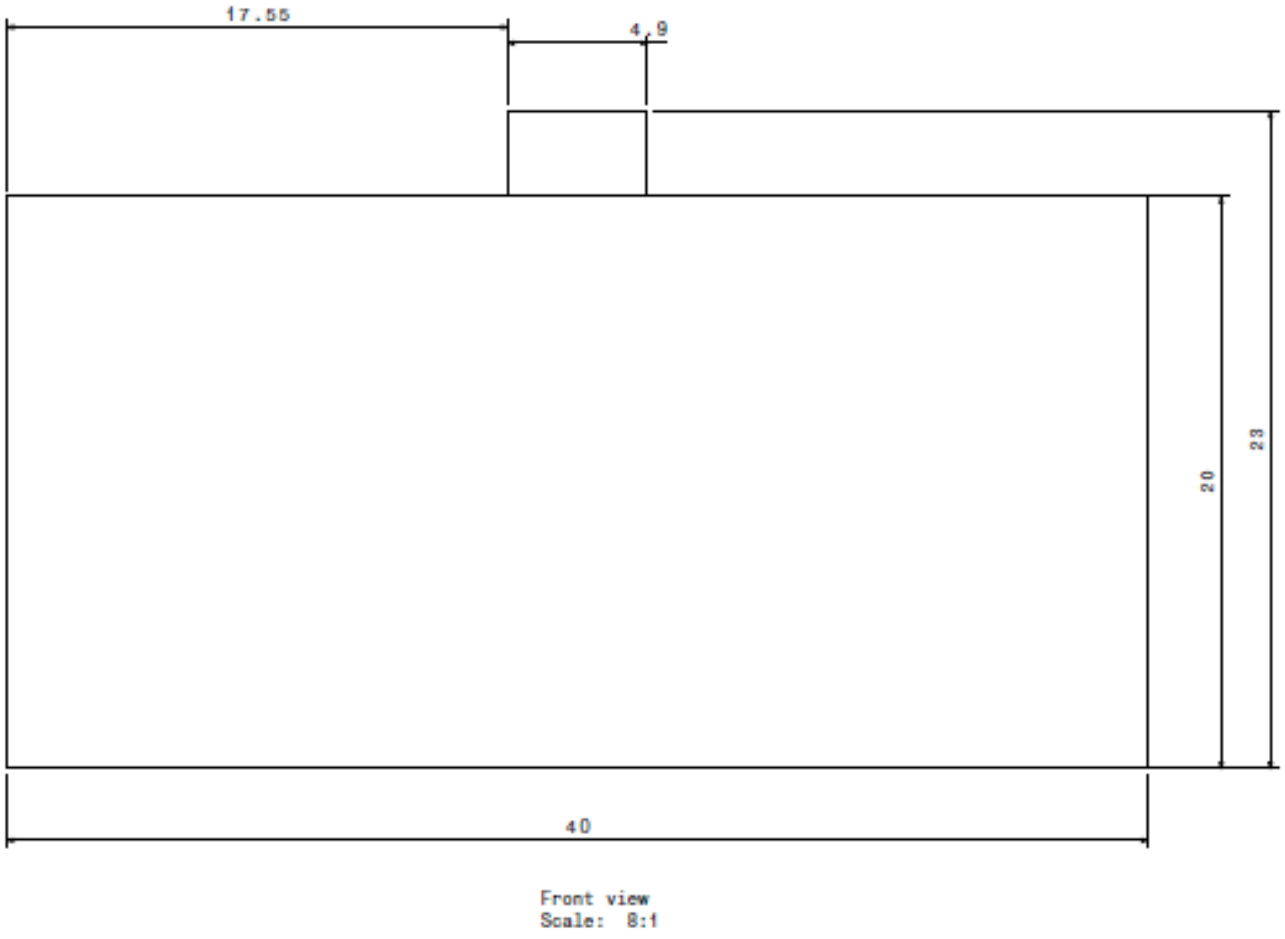

Fig. C.1 Drawing for the front view of the top layer sheet.

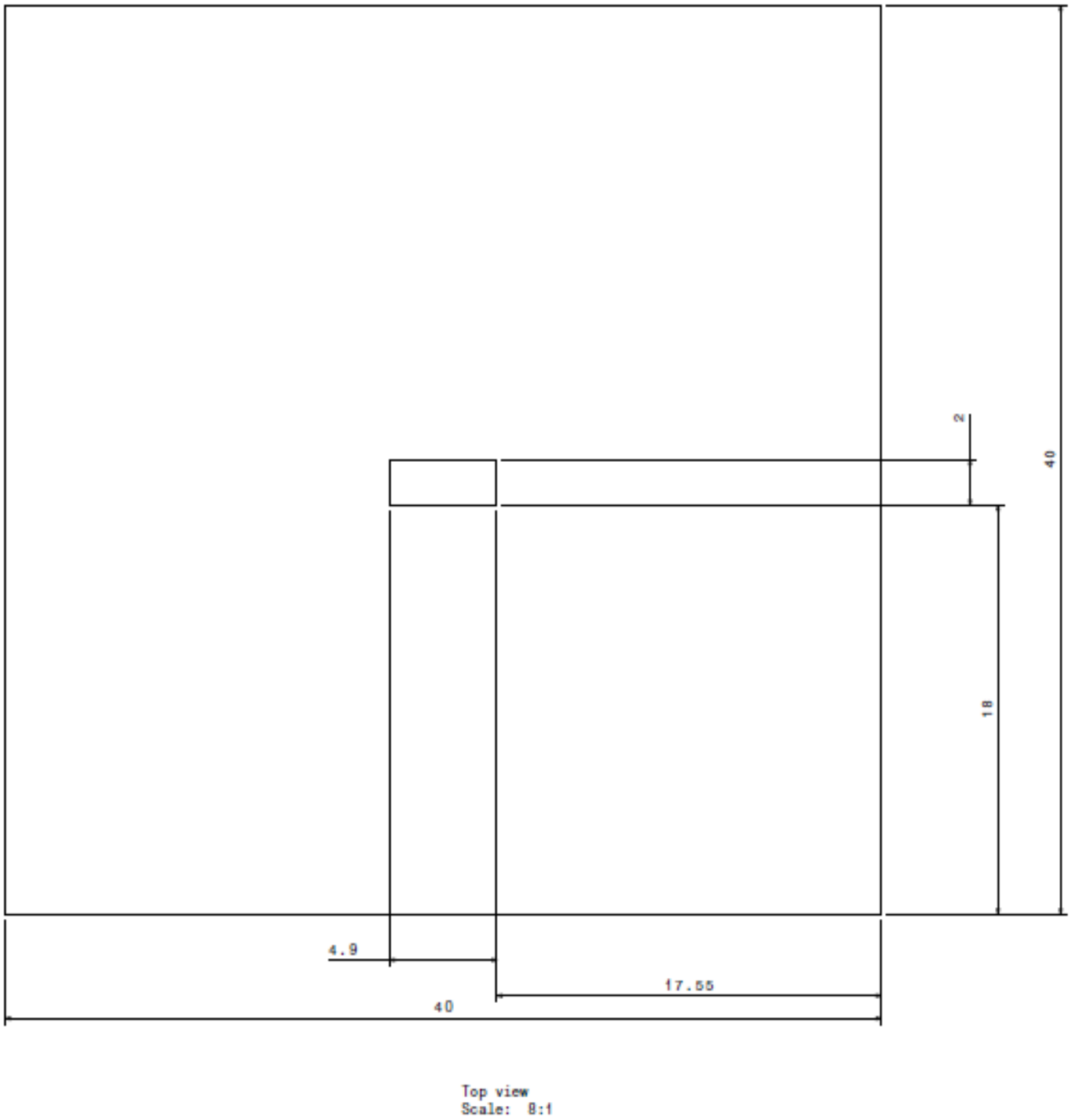

Fig. C.2 Drawing for the top view of the top layer sheet.

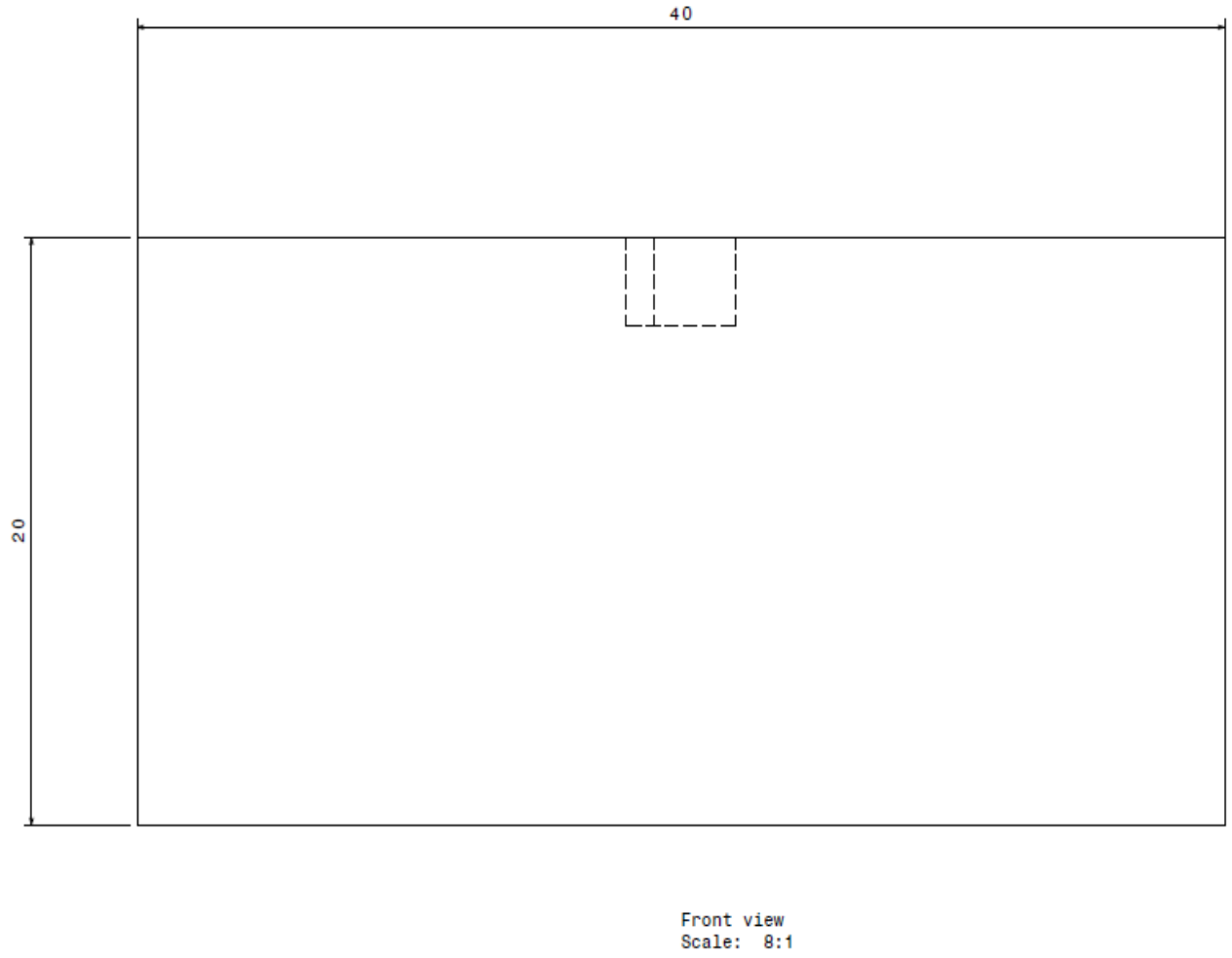

Fig. C.3 Drawing for the front view of the bottom layer sheet.

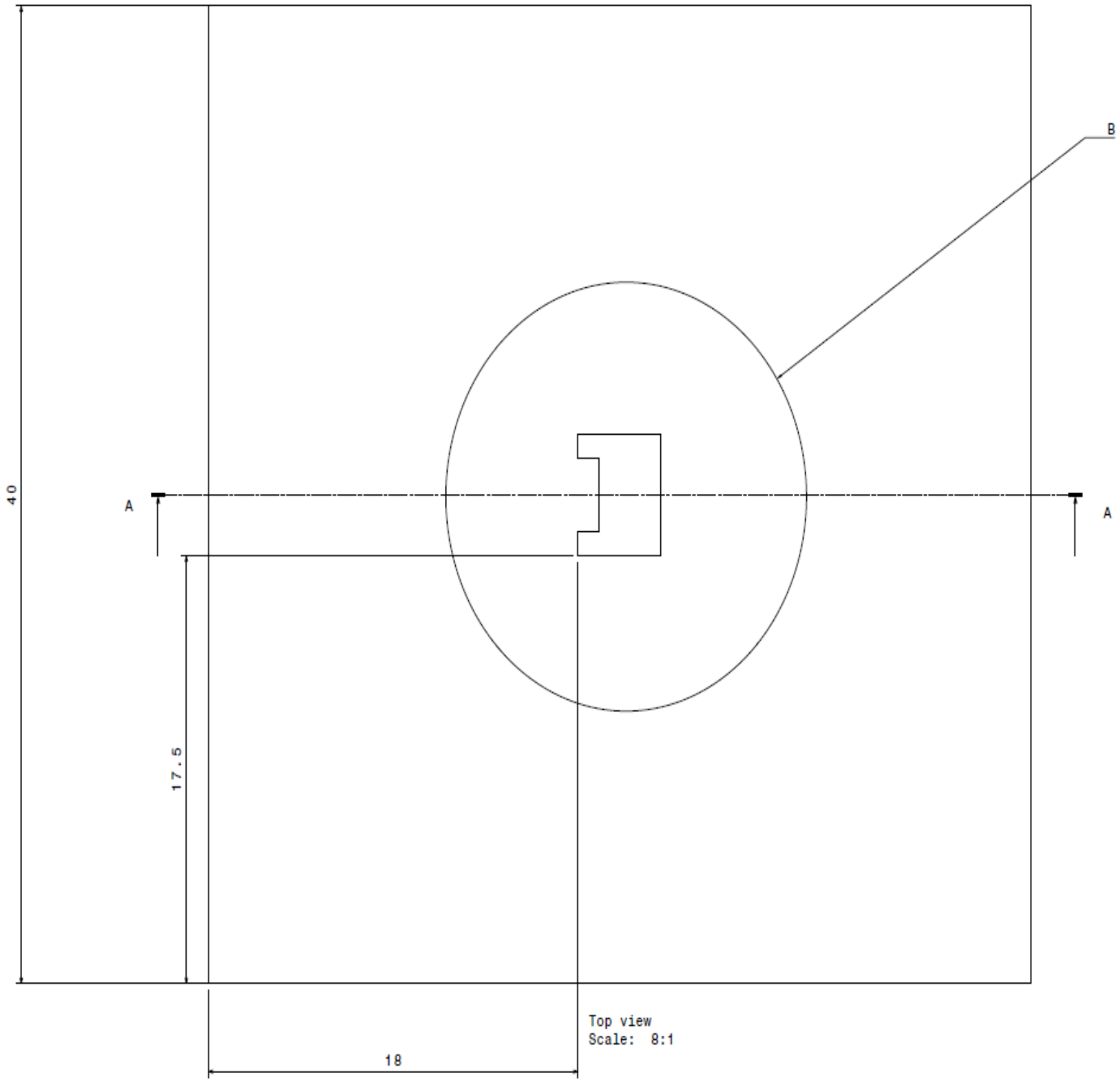

Fig. C.4 Drawing for the top view of the bottom layer sheet.

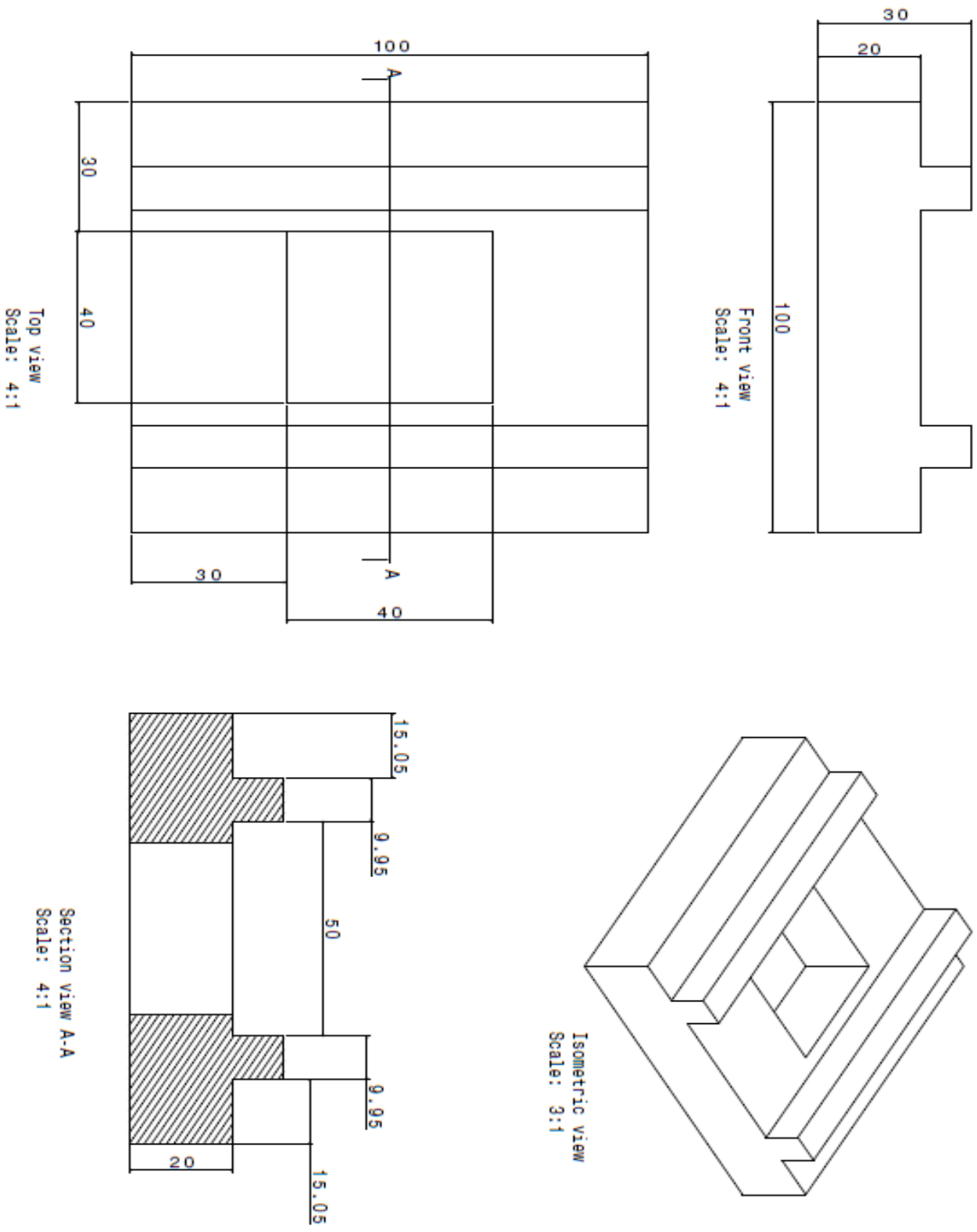

Fig. C.5 Drawings for the top block of sliding apparatus.

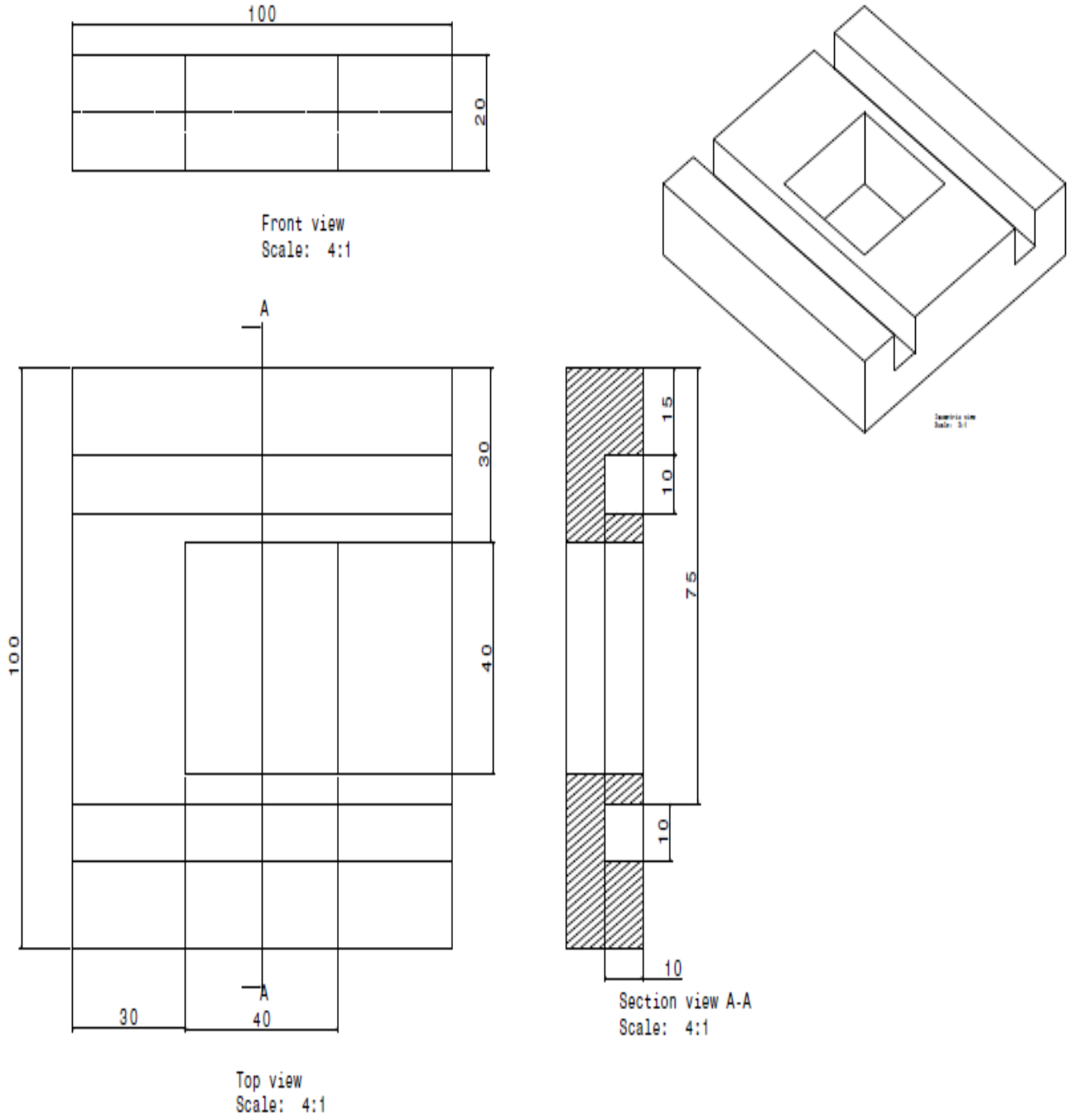

Fig. C.6 Drawings for the bottom block of sliding apparatus.